



3 1176 00139 1466

**NATIONAL ADVISORY COMMITTEE FOR AERONAUTICS**

# WARTIME REPORT

ORIGINALLY ISSUED

October 1943 as  
Advance Restricted Report 3J02

STRESSES AROUND RECTANGULAR CUT-OUTS IN SKIN-STRINGER

PANELS UNDER AXIAL LOADS - II

By Paul Kuhn, John E. Duberg, and Simon H. Diskin

Langley Memorial Aeronautical Laboratory  
Langley Field, Va.

NACA LIBRARY  
LANGLEY MEMORIAL AERONAUTICAL  
LABORATORY  
Langley Field, Va.

# NACA

WASHINGTON

NACA WARTIME REPORTS are reprints of papers originally issued to provide rapid distribution of advance research results to an authorized group requiring them for the war effort. They were previously held under a security status but are now unclassified. Some of these reports were not technically edited. All have been reproduced without change in order to expedite general distribution.

NATIONAL ADVISORY COMMITTEE FOR AERONAUTICS

---

ADVANCE RESTRICTED REPORT

---

STRESSES AROUND RECTANGULAR CUT-OUTS IN SKIN-STRINGER  
PANELS UNDER AXIAL LOADS - II

By Paul Kuhn, John E. Duberg, and Simon H. Diskin

SUMMARY

Cut-outs in wings or fuselages produce stress concentrations that present a serious problem to the stress analyst. As a partial solution of the general problem, this paper presents formulas for calculating the stress distribution around rectangular cut-outs in axially loaded panels. The formulas are derived by means of the substitute-stringer method of shear-lag analysis.

In a previous paper published under the same title as the present one, the analysis had been based on a substitute structure containing only two stringers. The present solution is based on a substitute structure containing three stringers and is more complete as well as more accurate than the previous one. It was found that the results could be used to improve the accuracy of the previous solution without appreciably reducing the speed of calculation. Details are given of the three-stringer solution as well as of the modified two-stringer solution.

L-368

In order to check the theory against experimental results, stringer stresses and shear stresses were measured around a systematic series of cut-outs. In addition, the stringer stresses measured in the previous investigation were reanalyzed by the new formulas. The three-stringer method was found to give very good accuracy in predicting the stringer stresses. The shear stresses cannot be predicted with a comparable degree of accuracy; the discrepancies are believed to be caused by local deformations taking place around the most highly loaded rivets and relieving the maximum shear stresses.

#### INTRODUCTION

Cut-outs in wings or fuselages constitute one of the most troublesome problems confronting the aircraft designer. Because the stress concentrations caused by cut-outs are localized, a number of valuable partial solutions of the problem can be obtained by analyzing the behavior, under load, of simple skin-stringer panels. A method for finding the stresses in axially loaded panels without cut-outs was given in reference 1, which also contained suggestions for estimating the stresses around cut-outs. In reference 2, these suggestions were put into more definite form as a set of formulas for analyzing an axially loaded panel with a cut-out (fig. 1).

L-368

Skin-stringer panels, although simpler than complete shells, are highly indeterminate structures. In order to reduce the labor of analyzing such panels, simplifying assumptions and special devices may be introduced. The most important device of this nature used in references 1 and 2 is a reduction of the number of stringers, which is effected by combining a number of stringers into a substitute single stringer. In reference 2, this reduction was carried to the extreme of using only two substitute stringers, one for the cut stringers and one for the uncut stringers, to represent one quadrant of the panel with a cut-out. The two-stringer structure can be analyzed very rapidly but, being somewhat over-simplified, cannot give an entirely satisfactory picture. In particular, the two-stringer structure does not include the region of the net section; and consequently this structure neither shows the effect of length of cut-out nor gives a solution for the maximum stringer stresses. These maximum stresses must be obtained by separate assumptions. In addition, there is no obvious relation between the shear stresses in the actual structure and the shear stresses in the substitute two-stringer structure as used in reference 2.

In order to obtain a more satisfactory basis of analysis than that of reference 2, formulas were developed for a

skin-stringer structure containing three stringers. At the same time, a new experimental investigation was made consisting of strain surveys around a systematic series of cut-outs. Stringer strains as well as shear strains in the sheet were measured in these tests, whereas only stringer strains had been measured in most of the tests of reference 2. A study of the three-stringer method and of the new experimental results indicated that the accuracy of the two-stringer method could be improved by introducing some modifications which have no appreciable effect on the rapidity of the calculations.

The main body of the present paper describes the application to a panel with a cut-out of a simplified three-stringer method of analysis as well as a modified two-stringer method. Comparisons are then shown between calculated and experimental results of the new tests and of the tests of reference 2. Appendixes A and B give mathematical details of the exact and of the simplified three-stringer methods, respectively. Appendix C gives a numerical example solved by all methods.

## THEORETICAL ANALYSIS OF CUT-OUTS IN AXIALLY LOADED SKIN-STRINGER PANELS

### General Principles and Assumptions

The general procedure of analysis is similar to the procedure developed for structures without cut-outs

L-368

(reference 1). The actual sheet-stringer structure is replaced by an idealized structure in which the sheet carries only shear. The ability of the sheet to carry normal stresses is taken into account by adding a suitable effective area of sheet to the cross-sectional area of each stringer. The idealized structure is then simplified by combining groups of stringers into single stringers, which are termed "substitute stringers"; this substitution is analogous to the use of "phantom members" in truss analysis. The substitute stringers are assumed to be connected by a sheet having the same properties as the actual sheet. The stresses in the substitute sheet-stringer structure are calculated by formulas obtained by solving the differential equations governing the problem. (See appendix A.) Finally, the stresses in the actual structure are calculated from the stresses in the substitute structure.

It will be assumed that the panel is symmetrical about both axes; the analysis can then be confined to one quadrant. It is furthermore assumed that the cross-sectional areas of the stringers and of the sheet do not vary spanwise, that the panel is very long, and that the stringer stresses are uniform at large spanwise distances from the cut-out.

6

### Symbols and Sign Conventions

- $A_1$  effective cross-sectional area of all continuous stringers, exclusive of main stringer bordering cut-out, square inches (fig. 2)
- $A_2$  effective cross-sectional area of main continuous stringer bordering cut-out, square inches (fig. 2)
- $A_3$  effective cross-sectional area of all discontinuous stringers, square inches (fig. 2)
- $A_{rib}$  cross-sectional area of rib at edge of cut-out, square inches (fig. 2)

$$B = \sqrt{\frac{K_1^2 + K_2^2 + 2\bar{K}}{K_1^2 + K_2^2 + 2\bar{K} - \frac{K_3 K_4}{K_1^2}}}$$

- $C$  stress-concentration factor (fig. 7)
- $C_0$  stress-excess factor for cut-out of zero length (fig. 3)

$$D = \lambda_1 + \lambda_2 = \sqrt{K_1^2 + K_2^2 + 2\bar{K}}$$

- $E$  Young's modulus of elasticity, kips per square inch
- $G$  shear modulus, kips per square inch

$$K^2 = \frac{Gt_2}{Eb_2} \left( \frac{1}{A_1 + A_2} + \frac{1}{A_3} \right)$$

$$K_1^2 = \frac{Gt_1}{Eb_1} \left( \frac{1}{A_1} + \frac{1}{A_2} \right)$$

$$K_2^2 = \frac{Gt_2}{Eb_2} \left( \frac{1}{A_2} + \frac{1}{A_3} \right)$$

$$K_3 = \frac{Gt_2}{Eb_1 A_2}$$

$$K_4 = \frac{Gt_1}{Eb_2 A_2}$$

$$\bar{K} = \sqrt{K_1^2 K_2^2 - K_3 K_4}$$

L half-length of cut-out, inches (fig. 2)

$$P_1 = \frac{K_1^2 (K_1^2 - \lambda_2^2)}{\lambda_1 (\lambda_1^2 - \lambda_2^2)}$$

$$P_2 = \frac{K_3 K_4}{\lambda_1 (\lambda_1^2 - \lambda_2^2)}$$

$$P_3 = \frac{K_1^2 (K_1^2 - \lambda_1^2)}{\lambda_2 (\lambda_1^2 - \lambda_2^2)}$$

$$P_4 = \frac{K_3 K_4}{\lambda_2 (\lambda_1^2 - \lambda_2^2)}$$

$Q_1$  force  $A_1 \bar{\sigma}$  acting on stringer 1 at rib, kips

$Q_2$  force  $A_2 \bar{\sigma}$  acting on stringer 2 at rib, kips

R stress-reduction factor to take care of change in length of cut-out (fig. 4)

L-368

8

$X_R$  difference between actual force in  $A_1$  (or  $A_2$ ) at the rib and the force  $Q_1$  (or  $Q_2$ ), kips

$a$  width of net section, inches (fig. 6)

$b$  half-width of cut-out, inches (fig. 6)

$b_1$  distance from  $A_2$  to centroid of  $A_1$  (fig. 2)

$b_2$  distance from  $A_2$  to centroid of  $A_3$  (fig. 2)

$$r_1 = - \frac{\tau_{2R} t_2}{A_3 \sigma_0}$$

$$r_2 = - \frac{\tau_{2R} t_2 - \tau_{1R} t_1}{A_2 (\sigma_{2R} - \sigma_0)}$$

$$r_3 = - \frac{G \sigma_{2R}}{E b_2 \tau_{2R}}$$

$t_1$  thickness of continuous panel, inches (fig. 2)

$t_2$  thickness of discontinuous panel, inches (fig. 2)

$x$  spanwise distances, inches (For origins, see figs. 2 and 6.)

$y$  chordwise distances, inches (For origins, see fig. 2.)

$$\lambda_1 = \sqrt{\frac{K_1^2 + K_2^2 + \sqrt{(K_1^2 + K_2^2)^2 - 4\bar{K}^2}}{2}}$$

$$\lambda_2 = \sqrt{\frac{K_1^2 + K_2^2 - \sqrt{(K_1^2 + K_2^2)^2 - 4\bar{K}^2}}{2}}$$

- L-368
- $\sigma_0$  average stress in the gross section, kips per square inch
- $\sigma_1$  stress in continuous substitute stringer, kips per square inch
- $\sigma_2$  stress in main continuous stringer, kips per square inch
- $\sigma_3$  stress in discontinuous substitute stringer, kips per square inch
- $\sigma_{rib}$  stress in rib, kips per square inch
- $\bar{\sigma}$  average stress in net section, kips per square inch
- $\tau_1$  shear stress in continuous substitute panel, kips per square inch
- $\tau_2$  shear stress in discontinuous substitute panel, kips per square inch

Superscripts on stresses denote forces producing the stresses. Subscript R denotes stress occurring at rib station.

Tensile stresses in stringers are positive. If the center line of cut-out is fixed, positive shear stresses are produced by a tensile force acting on  $A_1$ .

#### Simplified Three-Stringer Method

A principle for the effective use of substitute stringers was stated in reference 3 substantially as follows:

Leave the structure intact in the region of the stringer about which the most important actions take place, and replace the stringers away from this region by substitute stringers. In a panel with a cut-out, the most important action takes place around the main stringer bounding the cut-out. In accordance with the foregoing principle, the three-stringer method is based on retaining the main stringer as an individual stringer in the substitute structure; one substitute stringer replaces all the remaining continuous stringers, and another substitute stringer replaces all the discontinuous stringers. The three-stringer substitute structure obtained by this procedure is shown in figure 2, which summarizes graphically the salient features of the method. The figure shows the actual structure, the substitute structure, and the distribution of the stresses in the actual structure.

The maximum stringer stress as well as the maximum shear stress occurs at the rib station. The formulas given hereinafter for the stresses at the rib station and in the net section are based on the exact solution of the differential equations presented in appendix A. The formulas derived from this exact solution for the stresses in the gross section are somewhat cumbersome and are therefore replaced here by formulas that are based on mathematical

approximations of sufficient accuracy for design work (appendix B). The use of these approximations is the reason for calling this method the simplified three-stringer method.

Stresses at the rib station in the substitute structure.- The stringer stresses at the rib station are

$$\sigma_{1R} = \bar{\sigma} \left( 1 - \frac{RC_0 A_2}{A_1} \right) \quad (1)$$

$$\sigma_{2R} = \bar{\sigma} (1 + RC_0) \quad (2)$$

where the factor  $C_0$ , for a cut-out of zero length, is obtained from figure 3 and the factor  $R$ , which corrects  $C_0$  for length of cut-out, is obtained from figure 4. For practical purposes, the parameter  $B$  appearing in figure 4 may be assumed to equal unity. (See appendix A.) The length factor  $R$  depends, therefore, chiefly on the parameter  $K_1 L$ . This parameter is roughly equal to  $L/a$  for usual design proportions; in other words, the length effect can be related more directly to the length-width ratio  $L/a$  of the net section than to the proportions of the cut-out itself.

The running shear in the continuous panel at the rib station is

L-368

$$\tau_{1R} t_1 = - \bar{\sigma} RC_0 A_2 K_1 \tanh K_1 L \quad (3)$$

The running shear in the discontinuous panel at the rib station is

$$\tau_{2R} t_2 = - \bar{\sigma} A_2 \frac{K_4}{D} \left( 1 + RC_0 + \frac{K_1^2}{K} \right) \quad (4)$$

in which the factor  $D$  may be obtained from figure 5.

The stresses  $\sigma_{2R}$  and  $\tau_{2R}$  are the maximum values of  $\sigma_2$  and  $\tau_2$ , respectively, and are the maximum stresses in the panel. The stress  $\sigma_1$  reaches its maximum at the center line of the cut-out. The stress  $\tau_1$  reaches its maximum in the gross section at the station where

$$\sigma_1 = \sigma_2 \neq \sigma_0.$$

Stresses in the net section of the substitute structure.-

The formulas for the stresses in the net section are obtained from the exact solution (appendix A). At a distance  $x$  from the center line of the cut-out, the stresses in the continuous stringers are

$$\sigma_1 = \bar{\sigma} \left( 1 - \frac{RC_0 A_2 \cosh K_1 x}{A_1 \cosh K_1 L} \right)$$

$$\sigma_2 = \bar{\sigma} \left( 1 + RC_0 \frac{\cosh K_1 x}{\cosh K_1 L} \right)$$

As the length of the cut-out - or, more precisely, the

length of the net section - increases, the magnitude of the parameter  $K_1L$  increases and the stresses  $\sigma_1$  and  $\sigma_2$  converge toward the average stress  $\bar{\sigma}$  in the net section.

The running shear in the net section is

$$\tau_1 t_1 = -\bar{\sigma} R C_o A_2 K_1 \frac{\sinh K_1 x}{\cosh K_1 L}$$

and decreases rapidly to zero at the center line of the cut-out.

Stresses in the gross section of the substitute structure.- The stresses in the gross section can be obtained from the exact solution given in appendix A, but the formulas are too cumbersome for practical use. A simple approximate solution can, however, be derived (appendix B) that gives good accuracy in the immediate vicinity of the cut-out and reasonable accuracy at larger distances from the cut-out. The approximate solution assumes the differences between the stresses at the rib station and the average stresses in the gross section to decay exponentially with rate-of-decay factors adjusted to give the initial rates of decay of the exact solution.

The stress in the cut stringer by the approximate solution is

$$\sigma_3 = \sigma_o (1 - e^{-r_1 x}) \quad (5)$$

L-568

14

The stress in the main stringer is

$$\sigma_2 = \sigma_0 + (\sigma_{2R} - \sigma_0)e^{-r_2x} \quad (6)$$

The stress in the continuous stringer 1 follows from statics and is

$$\sigma_1 = \sigma_0 + \frac{A_2}{A_1} (\sigma_0 - \sigma_2) + \frac{A_3}{A_1} (\sigma_0 - \sigma_3) \quad (7)$$

The running shears in the sheet panels are

$$\tau_1 t_1 = \tau_{2R} t_2 e^{-r_1x} - (\tau_{2R} t_2 - \tau_{1R} t_1) e^{-r_2x} \quad (8)$$

$$\tau_2 t_2 = \tau_{2R} t_2 e^{-r_3x} \quad (9)$$

Stresses in the actual structure.- By the basic principles of the substitute structure, the stresses in the main continuous stringer of the actual structure are identical with the stresses in stringer 2 of the substitute structure; the total force in the remaining continuous stringers of the actual structure is equal to the force in stringer 1 of the substitute structure, and the total force in the cut stringers of the actual structure is equal to the force in stringer 3.

In the shear-lag theory for beams without cut-outs (reference 1), the force acting on a substitute stringer is distributed over the corresponding actual stringers on

L-368

the assumption that the chordwise distribution follows a hyperbolic cosine law. Inspection of the test data for panels with cut-outs indicated that neither this nor any other simple assumption fitted the data on the average as well as the assumption of uniform distribution. It is therefore recommended, for the present, that the stresses in all continuous stringers other than the main stringer be assumed to equal  $\sigma_1$  and that the stresses in all cut stringers be assumed to equal  $\sigma_3$ . (See fig. 2.) The validity of these assumptions will be discussed in connection with the study of the experimental data.

Again, by the principles of the substitute structure, the shear stresses  $\tau_1$  in the substitute structure equal the shear stresses in the first continuous sheet panel adjacent to the main stringer. In order to be consistent with the assumption that the chordwise distribution of the stringer stresses is uniform, the chordwise distribution of the shear stresses should be assumed to taper linearly from  $\tau_1$  to zero at the edge of the panel (fig. 2). Similarly, the chordwise distribution of the shear stresses in the cut sheet panels should be assumed to vary linearly from  $\tau_2$  adjacent to the main stringer to zero at the center line of the panel. Inspection of the test data indicated that this assumption does not hold very

well in the immediate vicinity of the cut-outs. The discrepancy is of some practical importance because the maximum stress in the rib depends on the chordwise distribution of the shear stress at the rib. By plotting experimental values, it was found that the law of chordwise distribution of the shear stress  $\tau_2$  at the rib station could be approximated quite well by a cubic parabola. The effect of this local variation may be assumed to end at a spanwise distance from the rib equal to one-fourth the full width of the cut-out. A straight line is sufficiently accurate to represent the spanwise variation within this distance (fig. 2).

If the stress  $\tau_2$  is distributed according to cubic law, the stress in the rib caused by the shear in the sheet is

$$\sigma_{rib} = \frac{\tau_{2R} t_2 b}{4k_{rib}} \left[ 1 - \left( \frac{y}{b} \right)^4 \right] \quad (10)$$

#### Modified Two-Stringer Method

The two-stringer method of analysis given in reference 2 is more rapid than, but not so accurate as, the three-stringer method previously described. It was found, however, that some improvements could be made, partly by incorporating some features of the three-stringer method, partly by other modifications.

L-368

The main features of the modified two-stringer method are summarized in figure 6. The cut stringers are replaced by a single substitute stringer; and all the uncut stringers, including the main one, are also replaced by a single stringer. Contrary to the usual shear-lag method, however, the stringer substituted for the continuous stringers is located not at the centroid of these stringers but along the edge of the cut-out. The substitute structure is used to establish the shear-lag parameter  $K$ , which determines the maximum shear stress, the spanwise rate of decay of the shear stress, and the spanwise rate of change of stringer stress. The maximum stringer stress must be obtained by an independent assumption, because a single stringer that is substituted for all continuous stringers obviously cannot give any indication of the chordwise distribution of stress in these stringers. No solutions are obtained by the two-stringer method for the shear stresses in the continuous panels, either in the net section or in the gross section.

Stresses in the substitute structure.- Throughout the length of the net section, the stress in the main stringer is

$$\sigma_{2R} = \bar{\sigma} [1 + 2R(C - 1)] \quad (11)$$

where  $C$  is the stress-concentration factor derived in

reference 2. Values of  $C$  may be obtained from figure 7, which is reproduced from reference 2 for convenience. It may be remarked here that reference 2 placed no explicit restriction on the use of the factor  $C$ ; whereas the use in formula (11) of the correction factor  $2R$ , which varies from 2 for short cut-outs to .1 for long cut-outs, implies that the factor  $C$  by itself should be used only when the net section is long.

In the gross section, the stress in the main stringer decreases with increasing distance from the rib according to the formula

$$\sigma_2 = \sigma_0 + (\sigma_{2R} - \sigma_0)e^{-Kx} \quad (12)$$

The stress in the discontinuous substitute stringer is

$$\sigma_3 = \sigma_0(1 - e^{-Kx}) \quad (13)$$

The stress  $\sigma_1$  may be obtained by formula (7) when  $\sigma_2$  and  $\sigma_3$  are known.

The running shear in the discontinuous panel is given by

$$\tau_2 t_2 = -\sigma_0 A_3 K e^{-Kx} \quad (14)$$

Stresses in the actual structure.- The stresses in the actual structure are obtained from the stresses in the substitute structure under the same assumptions as in the three-stringer method.

## EXPERIMENTAL VERIFICATION OF FORMULAS AND COMPARISON OF METHODS

### Test Specimens and Test Procedure

In order to obtain experimental verification for the formulas developed, a large skin-stringer panel was built and tested. The panel was similar to the one described in reference 2, but the scope of the tests was extended in two respects: Very short cut-outs were tested in addition to cut-outs of average length, and shear stresses as well as stringer stresses were measured around all cut-outs.

The general test setup is shown in figure 8. A setup of strain gages is shown in figure 9. The panel was made of 24S-T aluminum alloy and was 144 inches long. The cross section is shown in figure 10(a); figure 10(b) shows for reference purposes the cross section of the panel tested previously (reference 2). Strains were measured by Tuckerman strain gages with a gage length of 2 inches. The gages were used in pairs on both sides of the test panel. Strains were measured at corresponding points in all four quadrants. The final figures are drawn as for one quadrant; each plotted point represents, therefore, the average of four stations or eight gages.

The load was applied in three equal increments. If the straight line through the three points on the load-stress

L-368

plot did not pass through the origin, the line was shifted to pass through the origin; however, if the necessary shift was more than 0.2 kip per square inch, a new set of readings was taken.

An effective value of Young's modulus of  $10.16 \times 10^3$  kips per square inch was derived by measuring the strains in all stringers at three stations along the span before the first cut-out was made. This effective modulus may be considered as including corrections for the effects of rivet holes, average gage calibration factor, and dynamometer calibration factor. The individual gage factors were known to be within  $\pm \frac{1}{4}$  percent of the average.

The average strain at any one of the three stations in the panel without cut-out did not differ by more than 0.05 percent from the final total average. The maximum deviation of an individual stringer strain from the average was 5 percent; about 10 percent of the points deviated from the average by more than 3 percent. A survey was also made of longitudinal and transverse sheet strains at one station near the center. The average longitudinal sheet strain differed from the average stringer strain by 0.05 percent. The average transverse strain indicated a Poisson's ratio of 0.323.

### Discussion

L-368

The results of the tests are shown in figures 11 to 33. Calculated curves are given both for the exact three-stringer method and for the simplified three-stringer method. It may be recalled that either method assumes that the stresses in all continuous stringers except the main stringer have the magnitude  $\sigma_1$  and in all cut stringers, the magnitude  $\sigma_3$ . Because the values of  $\sigma_1$  and  $\sigma_3$  do not differ very much for the two methods, the curves for them computed by the simplified method are drawn only once in each figure.

A qualitative study of figures 11 to 32 indicates that the stress distribution calculated by the theory agrees sufficiently well with the experimental distribution to be acceptable for most stress-analysis purposes - in particular, the maximum stresses in each panel agree fairly well with the calculated ones. The most consistent discrepancies are chargeable to the simplifying assumption that the stringer stresses are identical in all the stringers represented by one substitute stringer. As a result of this assumption, the calculated stresses tend to be too low for the stringers close to the main stringer and too high for the stringers near the center line and near the edge of the panel. The fact that the calculated stresses for some of

the cut stringers are lower than the actual stresses is of little practical importance because these stringers would probably be designed to carry the stress  $\sigma_0$  rather than the actual stresses. On the uncut stringers, however, it may be necessary to allow some extra margin in the stringers near the main one. Aside from the consistent discrepancies just noted, figures 11 to 32 show that the stresses in the main stringers sometimes decrease spanwise more rapidly than the theory indicates. It is believed that this discrepancy also will seldom be of any consequence in practical analysis.

Of paramount interest to the analyst are the maximum values of the stresses. The quantitative study of errors in the maximum stresses is facilitated by table 1. The highest stresses occur theoretically at the rib station but, for practical reasons, measurements had to be made at some small distance from this line. The comparisons are made for the actual gage locations. The calculated values for the three-stringer method are based on the exact solution but, in the region of these gage locations, the exact solution and the simplified solution agree within a fraction of 1 percent.

The errors shown by table 1 for the maximum stringer stresses computed by the three-stringer method are but

L-368  
little larger than the local stress variations that were found experimentally to exist in the panel without cut-out. Presumably these variations are caused largely by failure of the rivets to enforce integral action of the structure.

The errors in the maximum shear stresses computed by the three-stringer method are consistently positive. The discrepancies are possibly caused by the sheet around the most highly loaded rivets deforming and thereby relieving the maximum shear stresses. The errors are higher than those on the stringer stresses and corrections to the theory appear desirable in some cases. The criterion that determines the accuracy of the theory cannot be definitely established from the tests. A rough rule appears to be that the error increases as the ratio of width of cut-out to width of panel decreases.

The errors given in table 1 for the two-stringer method show that this method is decidedly less accurate than the three-stringer method for computing maximum stringer stresses but that there is little difference between the two methods as far as the computation of the maximum shear stresses is concerned. A general study of the two theories indicates that this conclusion drawn from the tests is probably generally valid. It may be

recalled here that the two-stringer method gives no solution for shear stresses in the continuous panels.

Comparisons of the maximum observed rib stresses and the computed stresses are given in table 2. Two values of computed stress are shown. The smaller value was obtained on the assumption that the filler strips between the ribs and the sheet were effective in resisting the load applied to the ribs; whereas the larger value was obtained on the assumption that the filler strips were entirely ineffective. In figure 33, the chordwise variation of the observed and computed rib stresses is shown for three cut-outs. Because the chordwise distribution of shear stress in each sheet panel between two stringers is essentially constant, rib stresses computed by formula (10) will be too small when only a few stringers are cut. The computed values of rib stress were therefore determined by calculating the shear stress at the center of each panel according to the cubic law and assuming this shear stress to act in the whole panel.

The agreement between calculated and observed rib stresses is not all that could be desired. The discrepancy may be attributed to the approximation used for determining

the shear stresses and the uncertainty of the effective  
area of the rib.

Langley Memorial Aeronautical Laboratory,  
National Advisory Committee for Aeronautics,  
Langley Field, Va.

L-368

### APPENDIX A

#### EXACT SOLUTION OF THREE-STRINGER STRUCTURES

For a two-stringer panel constituting one half of a symmetrical structure, the application of the basic shear-lag theory yields the differential equation

$$\frac{d^2\tau}{dx^2} - K^2\tau = 0 \quad (A-1)$$

which is given in slightly different form in reference 4. In the analysis of a skin-stringer panel with a cut-out, a three-stringer substitute structure is used. (See fig. 2.) Application of the basic equations of reference 4 to a three-stringer structure yields in place of the single equation (A-1) the simultaneous equations

$$\left. \begin{aligned} \frac{d^2\tau_1}{dx^2} - K_1^2\tau_1 + K_3\tau_2 &= 0 \\ \frac{d^2\tau_2}{dx^2} - K_2^2\tau_2 + K_4\tau_1 &= 0 \end{aligned} \right\} \quad (A-2)$$

On the simplifying assumption that the panel is very long and that it is uniformly loaded by a stress  $\sigma_0$  at the far ends, the general solution of the equations (A-2) is

$$\tau_1 = c_1 e^{-\lambda_1 x} + c_2 e^{-\lambda_2 x} \quad (A-3)$$

$$\tau_2 = \left( \frac{K_1^2 - \lambda_1^2}{K_3} \right) c_1 e^{-\lambda_1 x} + \left( \frac{K_1^2 - \lambda_2^2}{K_3} \right) c_2 e^{-\lambda_2 x} \quad (A-4)$$

in which  $c_1$  and  $c_2$  are arbitrary constants.

L-368

Because the structure is assumed to be symmetrical about the longitudinal as well as the transverse axis, the analysis may be confined to one quadrant as shown in figure 34(a). The analysis can be simplified somewhat by severing the structure at the rib and considering separately the net section and the gross section. The solutions for the two-stringer structure representing the net section can be obtained from reference 4. The solutions for the three-stringer structure representing the gross section are obtained conveniently by considering two separate cases of loading. In the first case, stresses  $\sigma_0$  are assumed to be applied at the far end, and the stresses at the rib station are assumed to be uniform and equal to the average stress  $\bar{\sigma}$  necessary to balance the stresses  $\sigma_0$ . The forces at the rib station existing in the stringers are called the Q-forces (fig. 34(b)). In the second loading case, a group of two equal and opposite forces is assumed to load the stringers 1 and 2 at the rib station. These forces are called X-forces (fig. 34(c)).

In the net section the boundary conditions are as follows:

At  $x = 0$ ,

$$\tau_1 = 0 \quad (\text{from symmetry})$$

At  $x = L$ ,

$$\sigma_1 = - \frac{X_R}{A_1}$$

$$\sigma_2 = \frac{X_R}{A_2}$$

The substitution of these conditions in the solution of equation (A-1) yields

$$\tau_1^X = - \frac{X_R K_1}{t_1} \frac{\sinh K_1 x}{\cosh K_1 L} \quad (A-5)$$

$$\sigma_1^X = - \frac{X_R}{A_1} \frac{\cosh K_1 x}{\cosh K_1 L} \quad (A-6)$$

$$\sigma_2^X = \frac{X_R}{A_2} \frac{\cosh K_1 x}{\cosh K_1 L} \quad (A-7)$$

The superscript X indicates that the stresses are those caused by the action of the X-forces. In order to obtain the total stresses, the average stress  $\bar{\sigma}$  must be added to  $\sigma_1^X$  or  $\sigma_2^X$ . The shear stress  $\tau_1^X$  is the total stress because the uniform stress  $\bar{\sigma}$  is not accompanied by any shear stress.

When the Q-forces are applied to the gross section, the boundary conditions at  $x = 0$  are

$$\sigma_1 = \frac{Q_1}{A_1} = \bar{\sigma} \quad \sigma_2 = \frac{Q_2}{A_2} = \bar{\sigma} \quad \sigma_3 = 0$$

Applying these conditions to equations (A-3) and (A-4) gives the following solutions for stresses:

$$\tau_1^Q = \frac{Q_2}{t_1} (P_2 e^{-\lambda_1 x} - P_4 e^{-\lambda_2 x}) \quad (A-8)$$

$$\tau_2^Q = \frac{Q_2}{t_1} \left[ \frac{P_2 (K_1^2 - \lambda_1^2)}{K_3} e^{-\lambda_1 x} - \frac{P_4 (K_1^2 - \lambda_2^2)}{K_3} e^{-\lambda_2 x} \right] \quad (A-9)$$

$$\sigma_1^Q = \sigma_0 - \frac{Q_2}{A_1} \left( \frac{P_2}{\lambda_1} e^{-\lambda_1 x} - \frac{P_4}{\lambda_2} e^{-\lambda_2 x} \right) \quad (A-10)$$

$$\sigma_2^Q = \sigma_0 + \frac{Q_2}{A_2} \left\{ \frac{P_2}{\lambda_1} \left[ 1 - \frac{t_2 (K_1^2 - \lambda_1^2)}{t_1 K_3} \right] e^{-\lambda_1 x} - \frac{P_4}{\lambda_2} \left[ 1 - \frac{t_2 (K_1^2 - \lambda_2^2)}{t_1 K_3} \right] e^{-\lambda_2 x} \right\}$$

$$\sigma_3^Q = \sigma_0 + \frac{Q_2 t_2}{A_3 t_1} \left[ \frac{P_2}{\lambda_1} \frac{(K_1^2 - \lambda_1^2)}{K_3} e^{-\lambda_1 x} - \frac{P_4}{\lambda_2} \frac{(K_1^2 - \lambda_2^2)}{K_3} e^{-\lambda_2 x} \right]$$

The superscript Q indicates that the stresses are those caused by the action of the Q-forces.

The boundary conditions due to the application of the X-forces are, at  $x = 0$ ,

$$\sigma_1 = -\frac{X_R}{A_1} \quad \sigma_2 = \frac{X_R}{A_2} \quad \sigma_3 = 0$$

and the corresponding equations for stress are

$$\tau_1^X = \frac{X_R}{t_1} \left[ (P_1 + P_2) e^{-\lambda_1 x} - (P_3 + P_4) e^{-\lambda_2 x} \right] \quad (A-11)$$



For any length of cut-out,

$$X_R = Q_2 C_0 \frac{1}{1 + B \tanh K_1 L} = Q_2 C_0 R$$

where

$$B = \sqrt{\frac{K_1^2 + K_2^2 + 2\bar{K}}{K_1^2 + K_2^2 + 2\bar{K} - \frac{K_3 K_4}{K_1^2}}}$$

Values for  $C_0$  can be obtained from figure 3. In figure 4, the factor  $R$  is plotted for various values of  $K_1 L$  and  $B$ . The value of  $B$  may be assumed equal to unity with little loss in accuracy in the determination of stress; but, if a more exact solution is desired, the actual value of  $B$  may be computed and the curve in figure 4 corresponding to this value used.

APPENDIX B

SIMPLIFIED SOLUTION OF THREE-STRINGER STRUCTURES

The solutions for the stresses in the gross section given in appendix A are too involved for practical use, and a simplified method was developed. This method assumes that the differences between the values of  $\sigma_{2R}$ ,  $\sigma_{3R}$ , and  $\tau_{2R}$ , obtained by the exact solution, and the corresponding average stresses in the gross section decay exponentially with rate-of-decay factors adjusted to give initial rates of decay equal to those of the exact solution. These rates can be written simply in terms of the stresses at the rib and the properties of the panel. The solutions for  $\sigma_1$  and  $\tau_1$  are then derived from the solutions for  $\sigma_2$  and  $\sigma_3$ .

If it is assumed that the stresses in the cut stringer can be expressed by

$$\sigma_3 = \sigma_0(1 - e^{-r_1 x})$$

then

$$\frac{d\sigma_3}{dx} = \sigma_0 r_1 e^{-r_1 x}$$

but, from the basic shear-lag theory,

$$\frac{d\sigma_3}{dx} = -\frac{\tau_2 t_2}{A_3} = \sigma_0 r_1 e^{-r_1 x} \quad (B-1)$$

Therefore, at  $x = 0$ ,

$$r_1 = -\frac{\tau_{2R} t_2}{A_3 \sigma_0}$$

The stress in the main continuous stringer can be approximated by

$$\sigma_2 = \sigma_0 + (\sigma_{2R} - \sigma_0)e^{-r_2x}$$

which yields

$$\frac{d\sigma_2}{dx} = -(\sigma_{2R} - \sigma_0)r_2e^{-r_2x} \quad (B-2)$$

but, from the shear-lag theory,

$$\frac{d\sigma_2}{dx} = -\frac{\tau_1 t_1}{A_2} + \frac{\tau_2 t_2}{A_2} = -(\sigma_2 - \sigma_0)r_2e^{-r_2x}$$

Therefore, at  $x = 0$ ,

$$r_2 = -\frac{(\tau_{2R} t_2 - \tau_{1R} t_1)}{A_2(\sigma_{2R} - \sigma_0)}$$

The value of  $\sigma_1$  can be obtained by statics from  $\sigma_2$  and  $\sigma_3$  and is

$$\sigma_1 = \sigma_0 + \frac{A_2}{A_1} (\sigma_0 - \sigma_2) + \frac{A_3}{A_1} (\sigma_0 - \sigma_3) \quad (B-3)$$

If the value of  $\tau_2$  is assumed to decay exponentially, then

$$\tau_2 = \tau_{2R} e^{-r_3x}$$

and

$$\frac{d\tau_2}{dx} = -\tau_{2R} r_3 e^{-r_3x}$$

but, from the shear-lag theory,

$$\frac{d\tau_2}{dx} = \frac{G}{Eb_2} (\sigma_2 - \sigma_3) = -\tau_{2R} r_3 e^{-r_3x}$$

L-368

34

Therefore, at  $x = 0$ ,

$$\tau_3 = - \frac{G\sigma_{2R}}{Eb_2\tau_{2R}}$$

The shear stresses in the continuous panel can be determined from the rate of change of  $\sigma_1$ . From the shear-lag theory,

$$\frac{d\sigma_1}{dx} = \frac{\tau_1 t_1}{A_1} \quad (B-4)$$

Differentiation of formula (B-3) yields

$$\frac{d\sigma_1}{dx} = - \frac{A_3}{A_1} \frac{d\sigma_3}{dx} - \frac{A_2}{A_1} \frac{d\sigma_2}{dx} \quad (B-5)$$

Substitution of the derivatives (B-1) and (B-2) already obtained in (B-5) gives

$$\frac{d\sigma_1}{dx} = \frac{A_2}{A_1} (\sigma_{2R} - \sigma_o) r_2 e^{-r_2 x} - \frac{A_3}{A_1} \sigma_o r_1 e^{-r_1 x} \quad (B-6)$$

Finally, substitution of (B-6) in (B-4) yields

$$\tau_1 t_1 = \tau_{2R} t_2 e^{-r_1 x} - (\tau_{2R} t_2 - \tau_{1R} t_1) e^{-r_2 x}$$

APPENDIX C

NUMERICAL EXAMPLE

Analysis by the Exact Three-Stringer Method

The structure chosen for the numerical example is the 16-stringer panel tested as part of this investigation. The particular case chosen is the panel with eight stringers cut and with a length of cut-out equal to 30 inches. This cut-out is the one shown in figure 8. The cross section of the panel is shown in figure 10(a). The basic data are:

A <sub>1</sub> , sq in. . . . .	0.703
A <sub>2</sub> , sq in. . . . .	0.212
A <sub>3</sub> , sq in. . . . .	1.045
t <sub>1</sub> , in. . . . .	0.0331
t <sub>2</sub> , in. . . . .	0.0331
b <sub>1</sub> , in. . . . .	5.96
b <sub>2</sub> , in. . . . .	7.56
L, in. . . . .	15.0

These data yield the following values:

$$K_1^2 = 0.01295$$

$$K_2^2 = 0.00944$$

$$K_3 = 0.00995$$

$$K_4 = 0.00785$$

$$\bar{K} = 0.00664$$

From these parameters follow the factors for the rate of decay, which are

$$\lambda_1 = \sqrt{\frac{K_1^2 + K_2^2 + \sqrt{(K_1^2 + K_2^2)^2 - 4\bar{K}^2}}{2}} = 0.1421$$

$$\lambda_2 = \sqrt{\frac{K_1^2 + K_2^2 - \sqrt{(K_1^2 + K_2^2)^2 - 4\bar{K}^2}}{2}} = 0.0467$$

The computations of stress may more easily be made in terms of the constants  $P_1$ ,  $P_2$ ,  $P_3$ , and  $P_4$ , the values of which are

$$P_1 = \frac{K_1^2(K_1^2 - \lambda_2^2)}{\lambda_1(\lambda_1^2 - \lambda_2^2)} = \frac{0.01295(0.01295 - 0.00218)}{0.1421(0.02021 - 0.00218)} = 0.0545$$

$$P_2 = \frac{K_3 K_4}{\lambda_1(\lambda_1^2 - \lambda_2^2)} = \frac{0.00995 \times 0.00785}{0.1421(0.02021 - 0.00218)} = 0.0305$$

$$P_3 = \frac{K_1^2(K_1^2 + \lambda_1^2)}{\lambda_2(\lambda_1^2 - \lambda_2^2)} = \frac{0.01295(0.01295 + 0.02021)}{0.0467(0.02021 - 0.00218)} = -0.1117$$

$$P_4 = \frac{K_3 K_4}{\lambda_2(\lambda_1^2 - \lambda_2^2)} = \frac{0.00995 \times 0.00785}{0.0467(0.02021 - 0.00218)} = 0.0927$$

The reduced stress-excess factor is

$$\begin{aligned} RC_o &= \frac{P_4 - P_2}{P_1 + P_2 - P_3 - P_4 + K_1 \tanh K_1 L} \\ &= \frac{0.0927 - 0.0305}{0.0545 + 0.0305 + 0.1117 - 0.0927 + 0.1065} = 0.296 \end{aligned}$$

With a force of 7.5 kips acting on the half panel,

$$\sigma_o = \frac{7.50}{1.960} = 3.82 \text{ kips/sq in.}$$

and

$$\bar{\sigma} = \frac{7.50}{0.915} = 8.21 \text{ kips/sq in.}$$

Therefore,

$$X_R = RC_0 \bar{\sigma} A_2 = 0.296 \times 8.21 \times 0.212 = 0.514 \text{ kip}$$

Stresses in the net section.- The shear stress in the substitute panel of the net section is found by equation (A-5)

$$\begin{aligned} \tau_1 &= - \frac{X_R K_1}{t_1} \frac{\sinh K_1 x}{\cosh K_1 L} \\ &= - \frac{0.514 \times 0.1138}{0.0331} \frac{\sinh 0.1138x}{\cosh 1.707} \\ &= - 0.620 \sinh 0.1138x \end{aligned}$$

At the rib station,  $x = 15.0$  and

$$\tau_{1R} = -0.620 \sinh 1.707 = -1.65 \text{ kips/sq in.}$$

The stringer stresses are found by substituting in equations (A-6) and (A-7) and adding the average stress

$$\begin{aligned} \sigma_1 &= \bar{\sigma} - \frac{X_R}{A_1} \frac{\cosh K_1 x}{\cosh K_1 L} = 8.21 - \frac{0.514}{0.703} \frac{\cosh 0.1138x}{\cosh 1.707} \\ &= 8.21 - 0.257 \cosh 0.1138x \end{aligned}$$

$$\begin{aligned} \sigma_2 &= \bar{\sigma} + \frac{X_R}{A_2} \frac{\cosh K_1 x}{\cosh K_1 L} = 8.21 + \frac{0.514}{0.212} \frac{\cosh 0.1138x}{\cosh 1.707} \\ &= 8.21 + 0.850 \cosh 0.1138x \end{aligned}$$

L-368

38

The maximum stringer stress occurs in the main stringer at the rib,  $x = 15$ . The nearest gage location was at  $x = 13.5$ , where

$$\sigma_2 = 8.21 + 0.850 \cosh 1.536 = 8.21 + 2.05 = 10.26 \text{ kips/sq in.}$$

Stresses in the gross section.- The stresses in the gross section are obtained by adding the solutions for the stresses due to the X- and Q-forces. The shear stress in the continuous panel is obtained by adding equations (A-8) and (A-11). The final solution thus obtained is

$$\tau_1 = 2.92e^{-0.1421x} - 4.57e^{-0.0467x}$$

At the rib station,  $x = 0$  and

$$\tau_{1R} = 2.92 - 4.57 = -1.65 \text{ kips/sq in.}$$

This value of  $\tau_{1R}$  checks the one previously obtained for this same station in the net section.

Substituting the constants in equations (A-9) and (A-10) and combining gives

$$\tau_2 = -2.13e^{-0.1421x} - 4.95e^{-0.0467x}$$

At  $x = 1.50$ , the point of maximum observed shear stress,

$$\tau_2 = (-2.13)(0.809) - (4.95)(0.931) = -6.33 \text{ kips/sq in.}$$

The stress in the continuous substitute stringer is found by combining equations (A-10) and (A-12). The final result is

$$\sigma_1 = 3.82 - 0.97e^{-0.1421x} + 4.63e^{-0.0467x}$$

Similarly, the stresses in the main stringer and in the cut stringers are found by adding the proper values of the X- and Q-stresses. In the main stringer,

$$\sigma_2 = 3.82 + 5.55e^{-0.1421x} + 1.26e^{-0.0467x}$$

and, in the cut stringers,

$$\sigma_3 = 3.82 - 0.46e^{-0.1421x} - 3.36e^{-0.0467x}$$

Plots of the computed stresses in the panel for this cut-out are shown in figures 22 and 30.

Analysis by the Approximate Three-Stringer Method

The basic data are the same as for the exact three-stringer method. Compute

$$\frac{K_1^2 K_2^2}{K_3 K_4} = \frac{0.01295 \times 0.00944}{0.00995 \times 0.00785} = 1.565$$

$$\frac{\bar{K}}{K_2^2} = \frac{0.00664}{0.00944} = 0.704$$

From figure 3,

$$C_0 = 0.600$$

L-368

40

From figure 4 for  $K_1L = 1.707$  and the exact value of  $B = 1.10$ , there is obtained  $R = 0.492$ .

The stresses in the continuous stringers at the rib are, by formulas (1) and (2),

$$\sigma_{1R} = 8.21 \left[ 1 - (0.492)(0.600) \left( \frac{0.212}{0.703} \right) \right] = 7.48 \text{ kips/sq in.}$$

$$\sigma_{2R} = 8.21 \left[ 1 + (0.492)(0.600) \right] = 10.63 \text{ kips/sq in.}$$

The running shear in the continuous panel at the rib is, by formula (3),

$$\begin{aligned} \tau_{1R} t_1 &= -8.21 \times 0.492 \times 0.600 \times 0.212 \times 0.1138 \tanh 1.707 \\ &= -0.0547 \text{ kip/in.} \end{aligned}$$

The maximum running shear in the cut panel is computed by formula (4). The value of  $D$  is obtained from figure 5; with  $\bar{K} = 0.00664$  and  $K_1^2 + K_2^2 = 0.02239$ ,  $D = 0.189$  and

$$\begin{aligned} \tau_{2R} t_2 &= -8.21 \times 0.212 \times \frac{0.00785}{0.189} \left[ 1 + (0.492)(0.600) + \frac{0.01295}{0.00664} \right] \\ &= -0.234 \text{ kip/in.} \end{aligned}$$

$$\tau_{2R} = - \frac{0.234}{0.0331} = -7.08 \text{ kips/sq in.}$$

The stresses in the net section are computed as for the exact solution.

The rate-of-decay factors for the stresses in the gross section can now be computed

$$r_1 = - \frac{\tau_{2R} t_2}{A_3 \sigma_o} = - \frac{-0.234}{3.82 \times 1.045} = 0.0587$$

$$r_2 = - \frac{\tau_{2R} t_2 - \tau_{1R} t_1}{A_2 (\sigma_{2R} - \sigma_o)} = - \frac{-0.234 + 0.055}{0.212 (10.63 - 3.82)} = 0.1236$$

$$r_3 = - \frac{G_1 \sigma_{2R}}{E b_2 \tau_{2R}} = - \frac{0.380 \times 10.63}{7.56 \times -7.08} = 0.0755$$

The stress in the cut stringers by formula (5) is

$$\sigma_3 = 3.82 (1 - e^{-0.0587x})$$

and in the main stringer by formula (6) is

$$\sigma_2 = 3.82 + 6.93e^{-0.1236x}$$

The stress in the continuous stringer can be found by formula (7).

The running shears are, by formulas (8) and (9),

$$\tau_1 t_1 = -0.234e^{-0.0587x} + 0.179e^{-0.1218x}$$

$$\tau_2 t_2 = -0.234e^{-0.0755x}$$

At  $x = 1.50$ , the point of maximum observed shear stress,

$$\begin{aligned} \tau_2 t_2 &= -0.234 \times 0.893 \\ &= -0.209 \text{ kip/in.} \end{aligned}$$

L-363

42

and

$$\begin{aligned} \tau_2 &= - \frac{0.209}{0.0331} \\ &= -6.31 \text{ kips/sq in.} \end{aligned}$$

Analysis by the Two-Stringer Solution

The basic data remain as before. Compute

$$\begin{aligned} \frac{a}{b} &= \frac{9.38}{14.06} \\ &= 0.667 \end{aligned}$$

$$\begin{aligned} \frac{aA_3}{b(A_1 + A_2)} &= \frac{1.045 \times 9.38}{14.06 \times 0.915} \\ &= 0.764 \end{aligned}$$

Then from figure 7 is obtained

$$C = 1.195$$

The maximum stringer stress can then be computed by formula (11)

$$\begin{aligned} \sigma_{2R} &= 8.21 [1 + 2(0.492)(0.195)] \\ &= 9.65 \text{ kips/sq in.} \end{aligned}$$

By statics,

$$\sigma_{1R} = 7.70 \text{ kips/sq in.}$$

The rate-of-decay factor is computed from

$$\begin{aligned} K^2 &= \frac{0.380 \times 0.0331}{7.56} \left( \frac{1}{0.915} + \frac{1}{1.045} \right) \\ &= 0.00342 \end{aligned}$$

$$K = 0.0585$$

In the net section the stringer stresses are assumed to be constant and equal to the stresses at the rib. For the gross section, by formula (12), the stress in the main stringer is

$$\sigma_2 = 3.82 + 6.03e^{-0.0585x}$$

and, by formula (13), the stress in the discontinuous stringers is

$$\sigma_3 = 3.82(1 - e^{-0.0585x})$$

The stress in the continuous stringers may be found by using formula (7).

The running shear in the cut panel is, by formula (14),

$$\begin{aligned}\tau_2 t_2 &= -3.82 \times 1.045 \times 0.0585e^{-0.0585x} \\ &= -0.234e^{-0.0585x}\end{aligned}$$

At  $x = 1.50$ , the point of maximum observed shear stress,

$$\begin{aligned}\tau_2 t_2 &= -0.0234 \times 0.916 \\ &= -0.214 \text{ kip/in.}\end{aligned}$$

and

$$\begin{aligned}\tau_2 &= -\frac{0.214}{0.0331} \\ &= -6.47 \text{ kips/sq in.}\end{aligned}$$

REFERENCES

1. Kuhn, Paul, and Chiarito, Patrick T.: Shear Lag in Box Beams - Methods of Analysis and Experimental Investigations. Rep. No. 739, NACA, 1942.
2. Kuhn, Paul, and Moggio, Edwin M.: Stresses around Rectangular Cut-Outs in Skin-Stringer Panels under Axial Loads. NACA A.R.R., June 1942.
3. Kuhn, Paul: Approximate Stress Analysis of Multi-stringer Beams with Shear Deformation of the Flanges. Rep. No. 636, NACA, 1938.
4. Kuhn, Paul: Stress Analysis of Beams with Shear Deformation of the Flanges. Rep. No. 608, NACA, 1937.

TABLE 1

COMPARISON OF OBSERVED AND CALCULATED MAXIMUM STRESSES

NACA

Number of stringers		Half-length cut-out (in.)	Load on panel (kips)	Stringer stresses						Shear stresses			
				Observed maximum stress (kips/sq in.)	Three-stringer solution		Two-stringer solution		Observed maximum stress (kips/sq in.)	Three-stringer solution		Two-stringer solution	
					Calculated (kips/sq in.)	Error (percent) (a)	Calculated (kips/sq in.)	Error (percent) (a)		Calculated (kips/sq in.)	Error (percent) (a)	Calculated (kips/sq in.)	Error (percent) (a)
Total	Cut												
16-stringer test panel, length = 144.0 in.													
16	2	1.5	15.0	6.82	7.02	2.9	7.76	13.8	-2.97	-3.91	31.7	-3.85	29.6
16	4	1.5	15.0	8.69	8.86	1.9	8.52	-2.0	-4.19	-5.03	20.1	-4.71	12.4
16	6	1.5	15.0	10.71	10.49	-2.1	9.50	-11.3	-5.34	-5.90	10.5	-5.47	2.4
16	8	1.5	15.0	13.20	12.33	-6.6	10.90	-17.4	-6.55	-6.68	1.9	-6.47	-1.2
16	8	8.0	15.0	11.00	10.63	-3.4	10.00	-9.1	-6.00	-6.40	6.6	-6.47	7.8
16	8	15.0	15.0	10.37	10.26	-1.1	9.85	-5.0	-5.90	-6.33	7.4	-6.47	9.7
16	10	15.0	15.0	13.30	13.14	-1.2	12.80	-3.9	-7.20	-7.62	5.9	-7.73	7.4
16	12	15.0	15.0	19.61	19.34	-1.4	19.43	-0.9	-9.41	-9.77	3.9	-9.80	4.1
15-stringer test panel, length = 141.6 in.													
15	1	8.3	8.94	3.56	3.67	3.2	4.60	29.5	-----	-----	-----	-----	-----
15	3	8.3	8.94	4.74	4.76	.4	5.19	9.5	-----	-----	-----	-----	-----
15	5	8.3	8.94	5.82	5.71	-2.0	5.72	-1.7	-----	-----	-----	-----	-----
15	7	8.3	8.94	7.08	6.79	-4.1	6.70	-5.4	-----	-----	-----	-----	-----
15	9	8.3	8.94	9.02	8.36	-7.3	8.23	-8.8	-----	-----	-----	-----	-----
15	b9	8.3	10.85	5.83	5.92	1.5	6.31	8.2	-----	-----	-----	-----	-----
7- and 8-stringer test panels, length = 62.5 in.													
7	1	5.0	20.0	18.85	18.39	-2.4	21.40	13.5	19.20	19.70	2.5	19.40	1.0
7	3	5.0	20.0	29.40	27.95	-5.3	29.00	-1.4	12.40	12.80	3.2	13.50	8.9
8	2	5.0	20.0	20.25	19.21	-5.4	21.30	5.2	16.80	19.70	17.3	19.80	17.8
8	4	5.0	20.0	30.60	27.91	-8.8	29.60	-3.3	8.60	10.60	23.3	10.20	15.7
Average of absolute errors for all tests													
						3.4		8.3			11.2		9.8

<sup>a</sup> Errors are  $\frac{\text{Calculated} - \text{Observed}}{\text{Observed}} \times 100$ .

<sup>b</sup> Area of main stringer increased.

**TABLE 2**

**COMPARISON OF OBSERVED AND CALCULATED MAXIMUM RIB STRESSES**  
 [Load on panel, 15 kips]

L-360

Number of stringers		Half-length cut-out (in.)	Observed stresses (kips/sq in.)	Calculated stresses (kips/sq in.)	
Total	Cut			(a)	(b)
16	2	1.5	1.57	2.51	1.48
16	4	1.5	2.20	3.29	1.94
16	6	1.5	2.73	4.42	2.60
16	8	1.5	2.89	5.73	3.38
16	8	8.0	4.30	3.32	2.91
16	8	15.0	4.77	3.28	2.88
16	10	15.0	5.49	4.48	3.94
16	12	15.0	6.75	6.49	5.70

<sup>a</sup>Filler strips ineffective.

<sup>b</sup>Filler strips effective.

NACA

Fig. 1

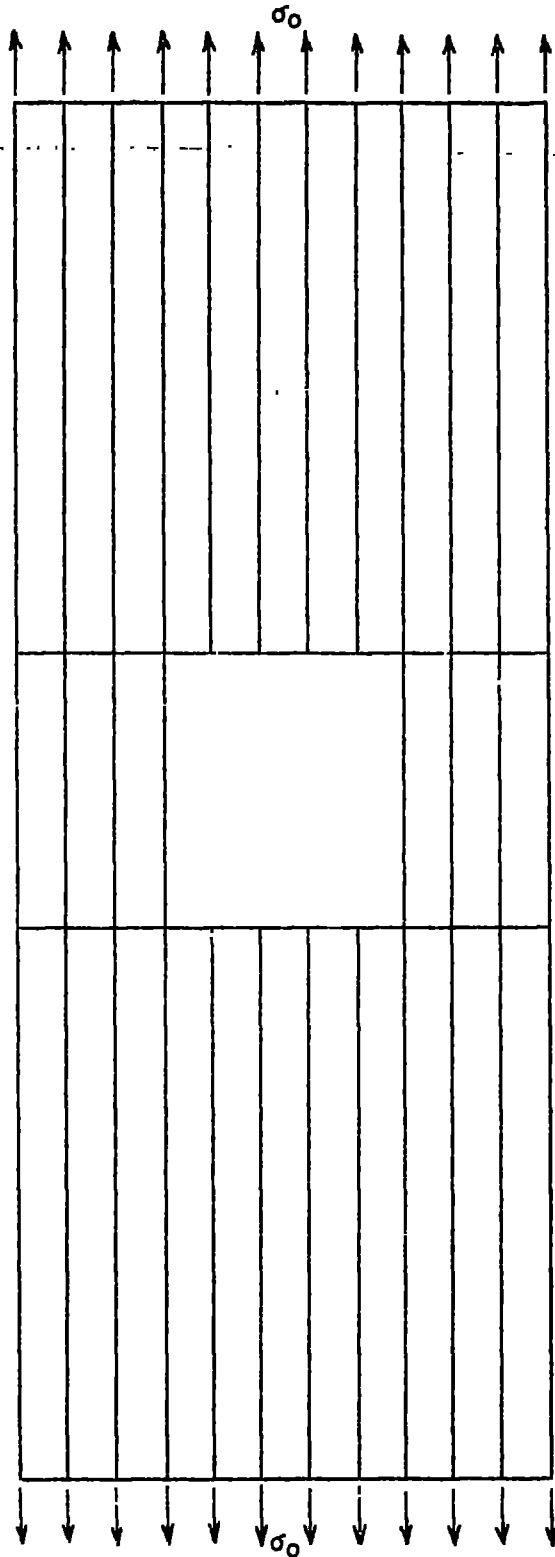


Figure 1.- Axially loaded panel with cut-out.



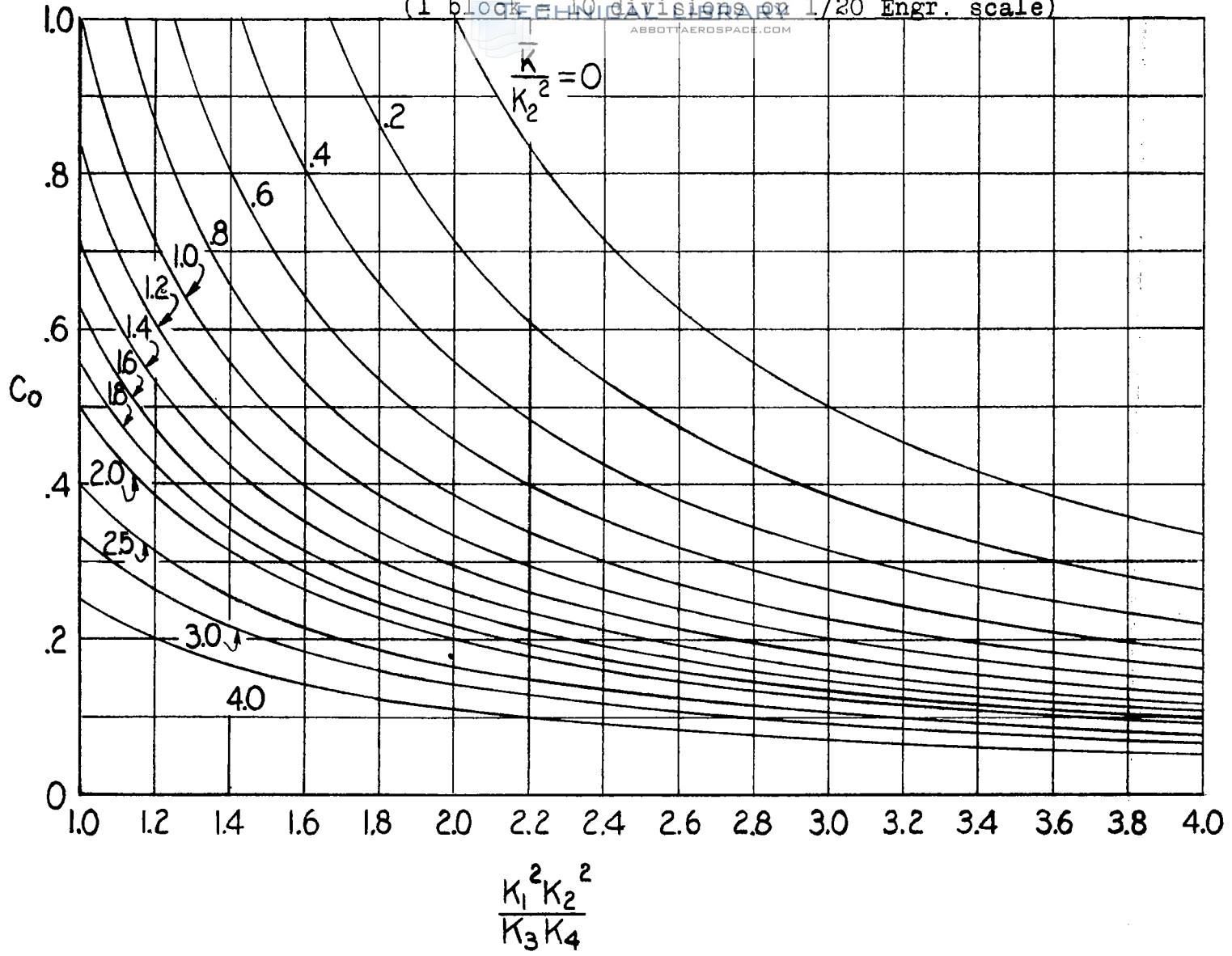


Figure 3. - Graph for factor  $C_0$ .

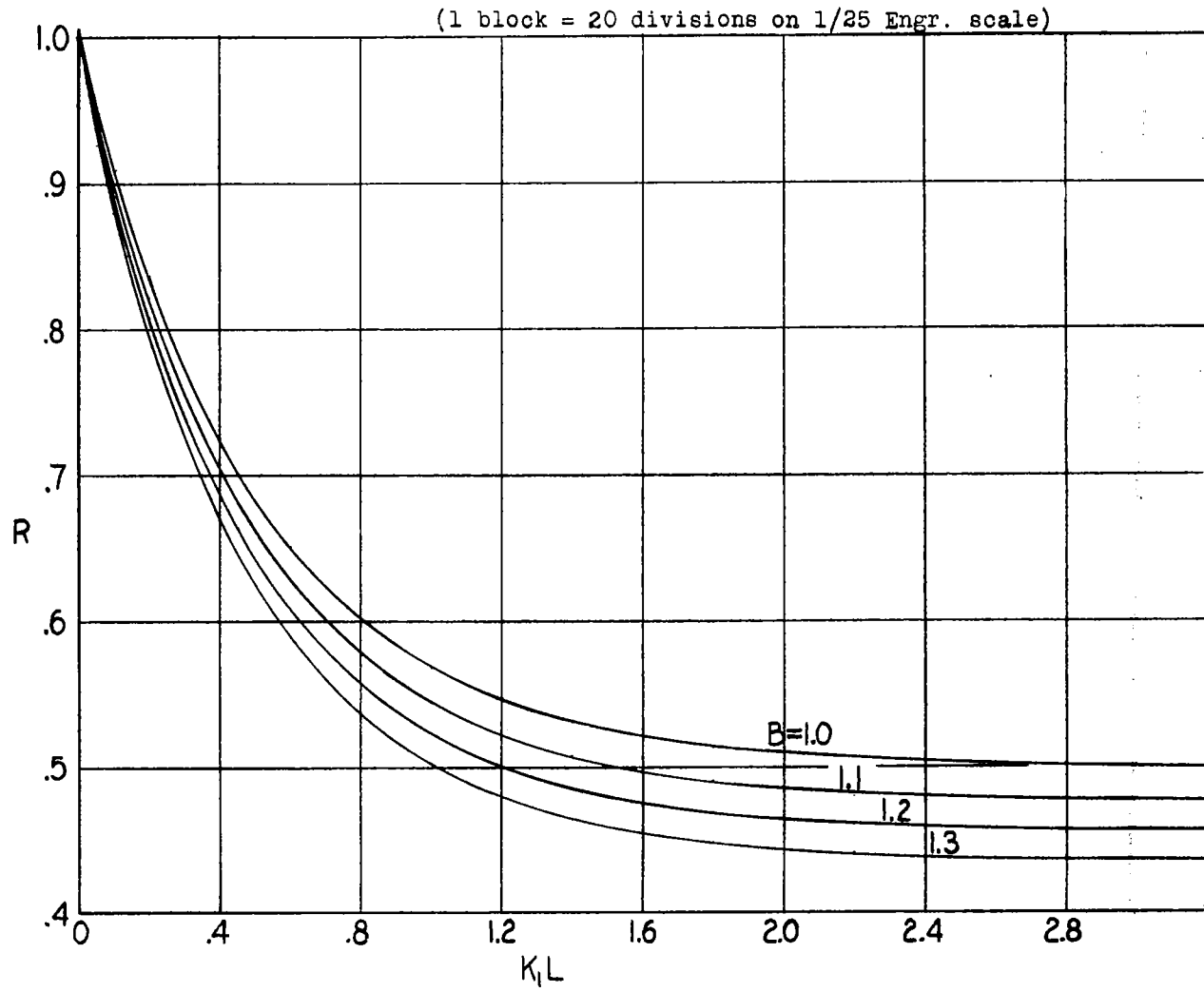


Figure 4. - Graph for factor R.

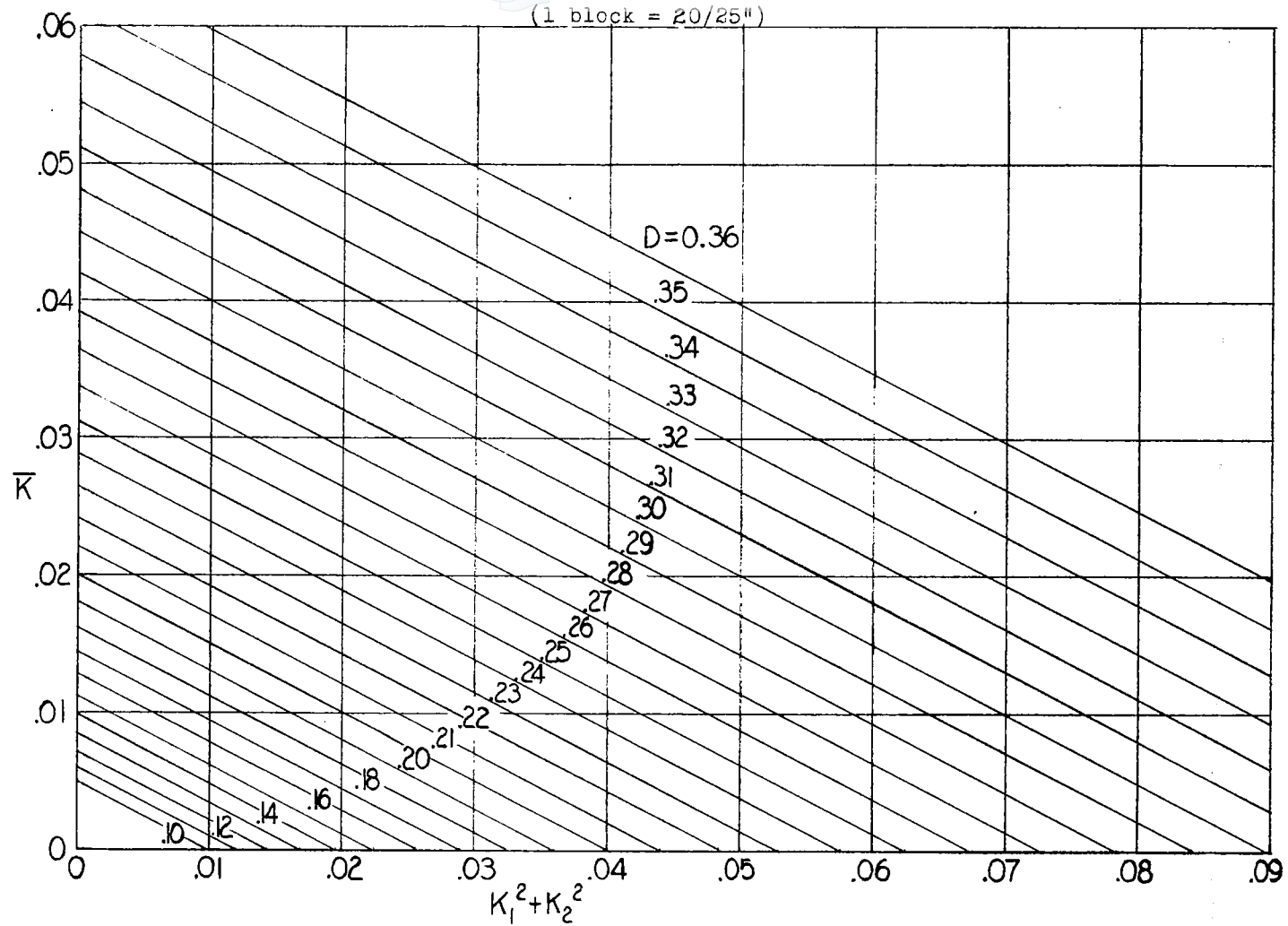


Figure 5.-Graph for factor D.

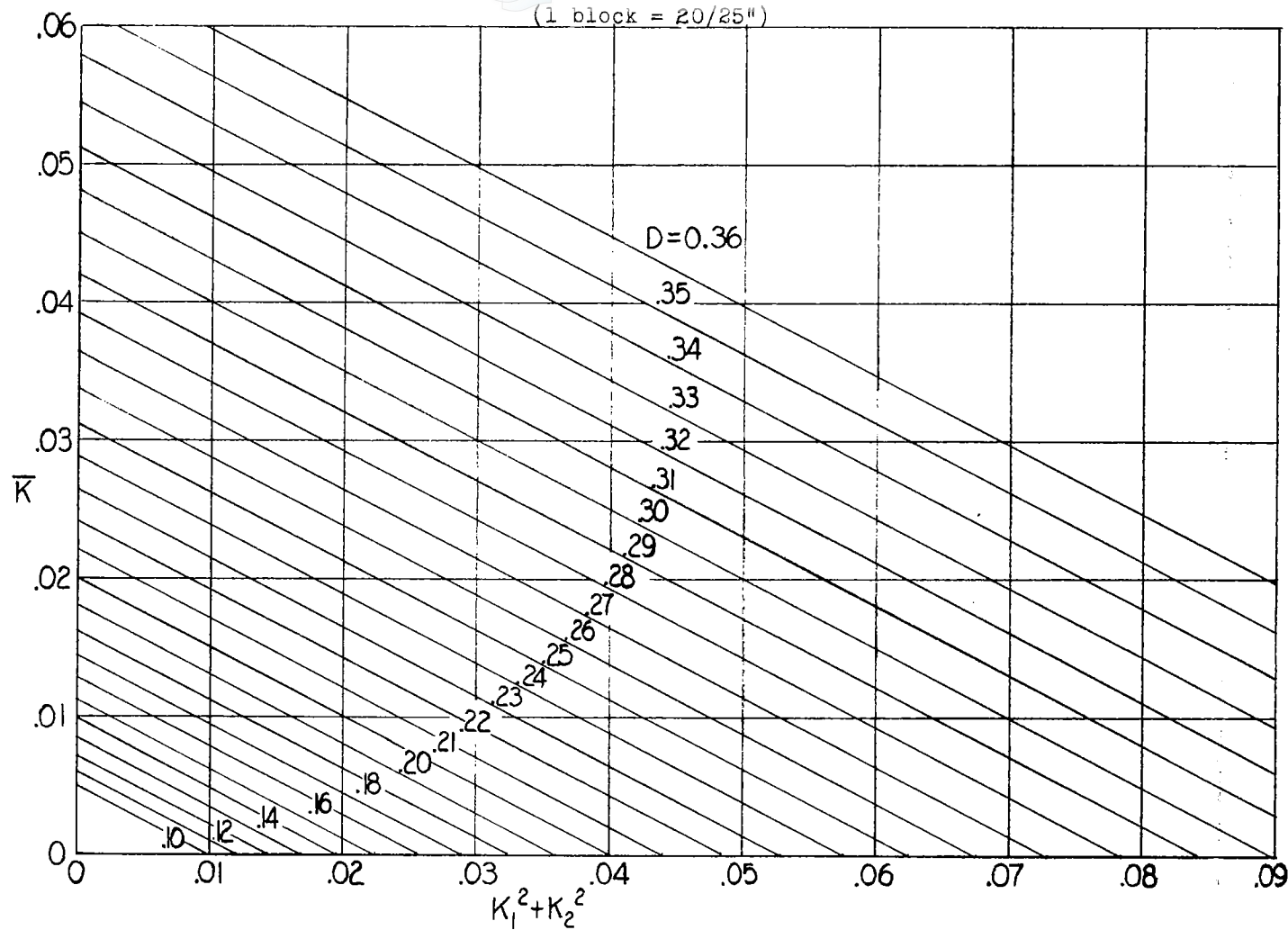


Figure 5.-Graph for factor D.

NACA

Fig. 6

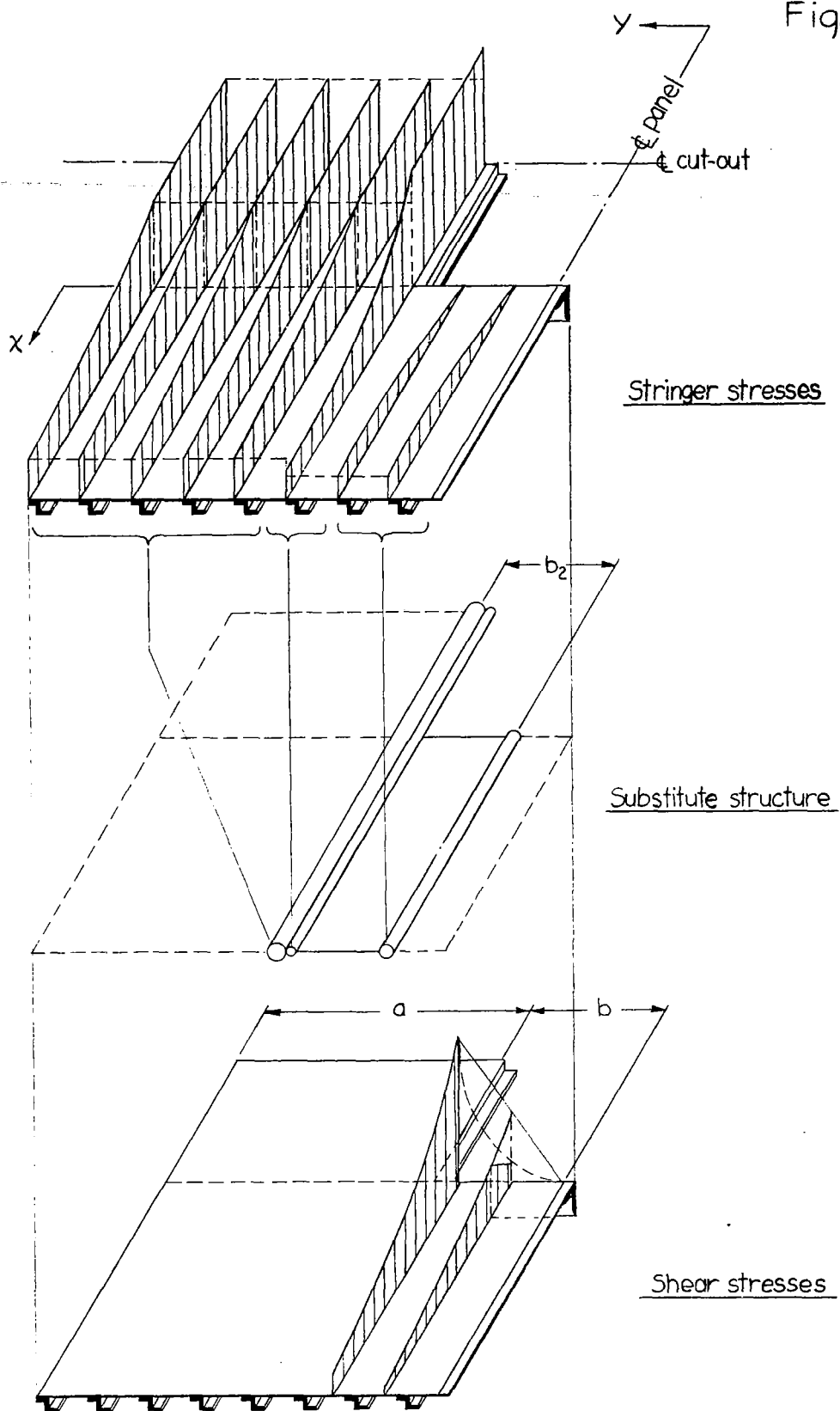


Figure 6-Stress distribution around cut-out by modified two-stringer method.

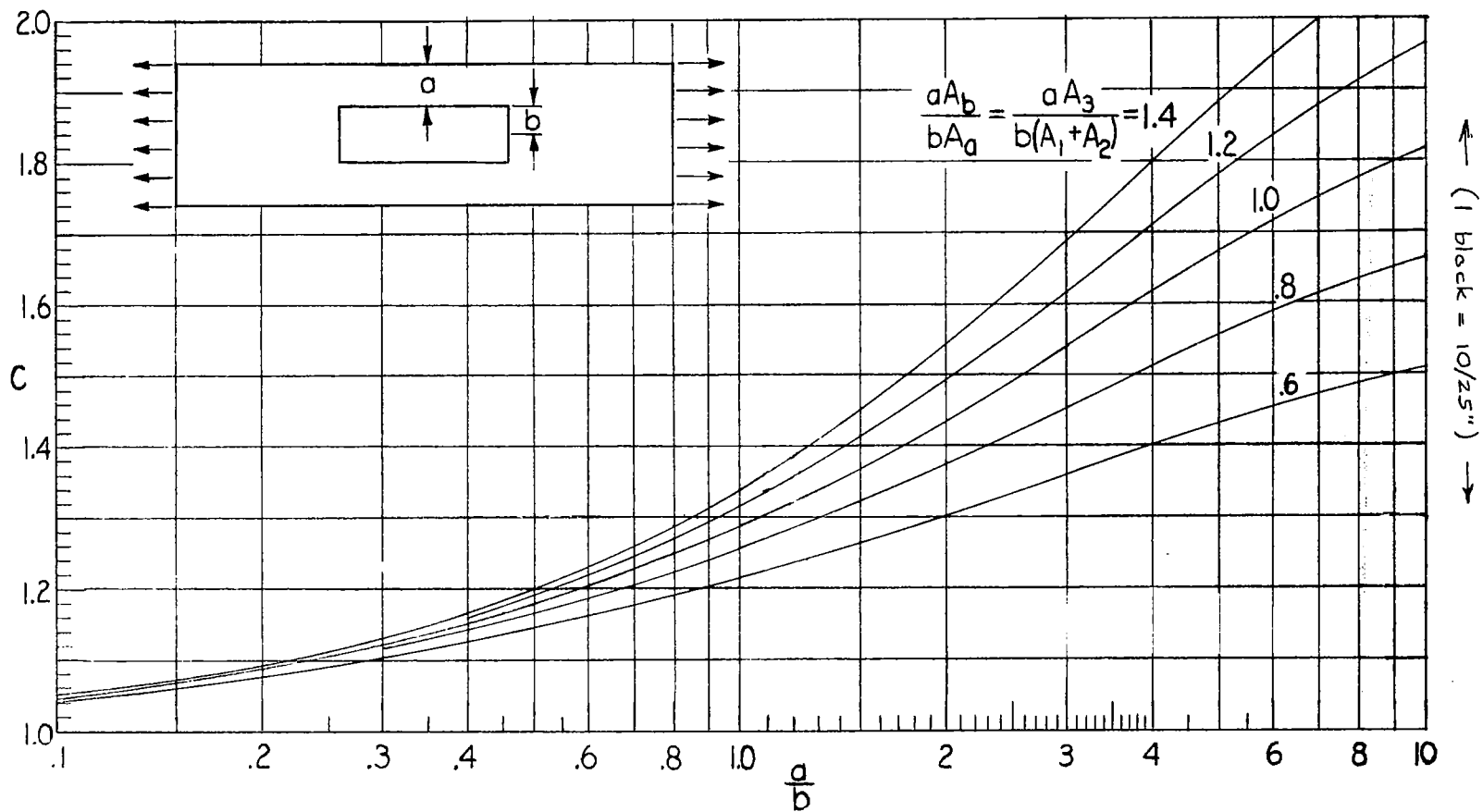


Figure 7.- Approximate stress-concentration factor  $C$  for stringer stresses (from reference 2).



Figure 8.- Test set-up on 16-stringer panel with eight stringers cut and  $L = 15$  in.

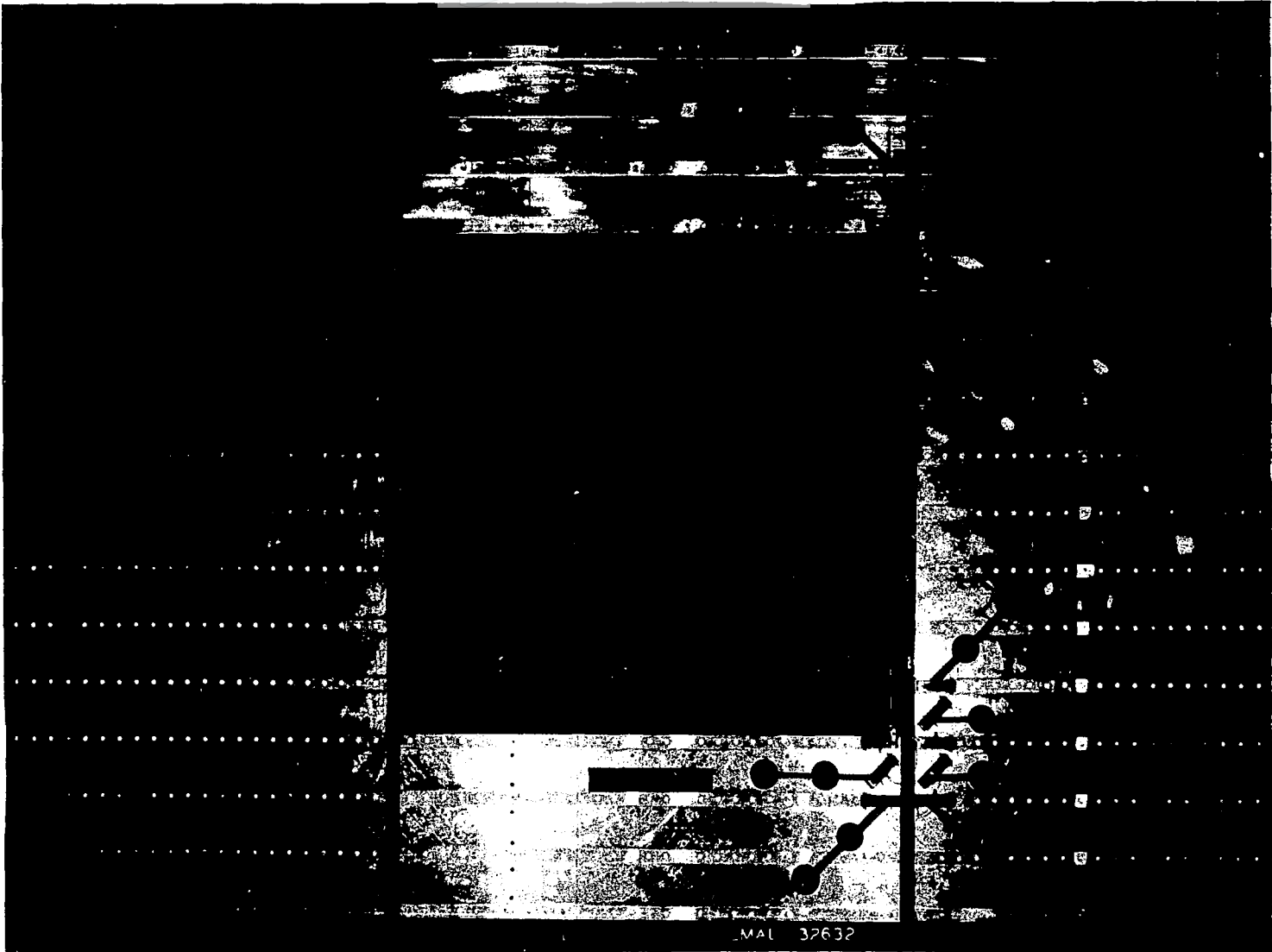


Figure 9... Typical set-up of strain gages.

NACA

FIG. 9

NACA

Figs. 10,11

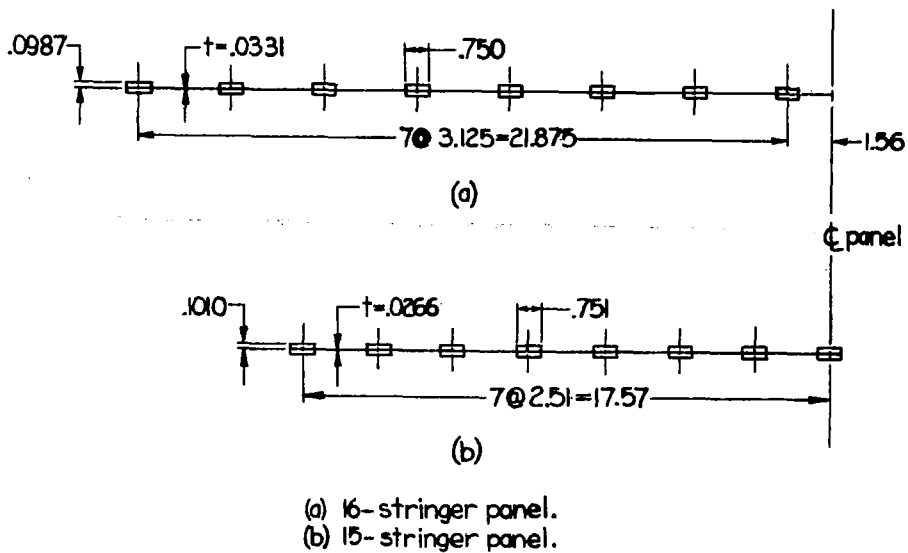


Figure 10.- Cross sections of test panels.

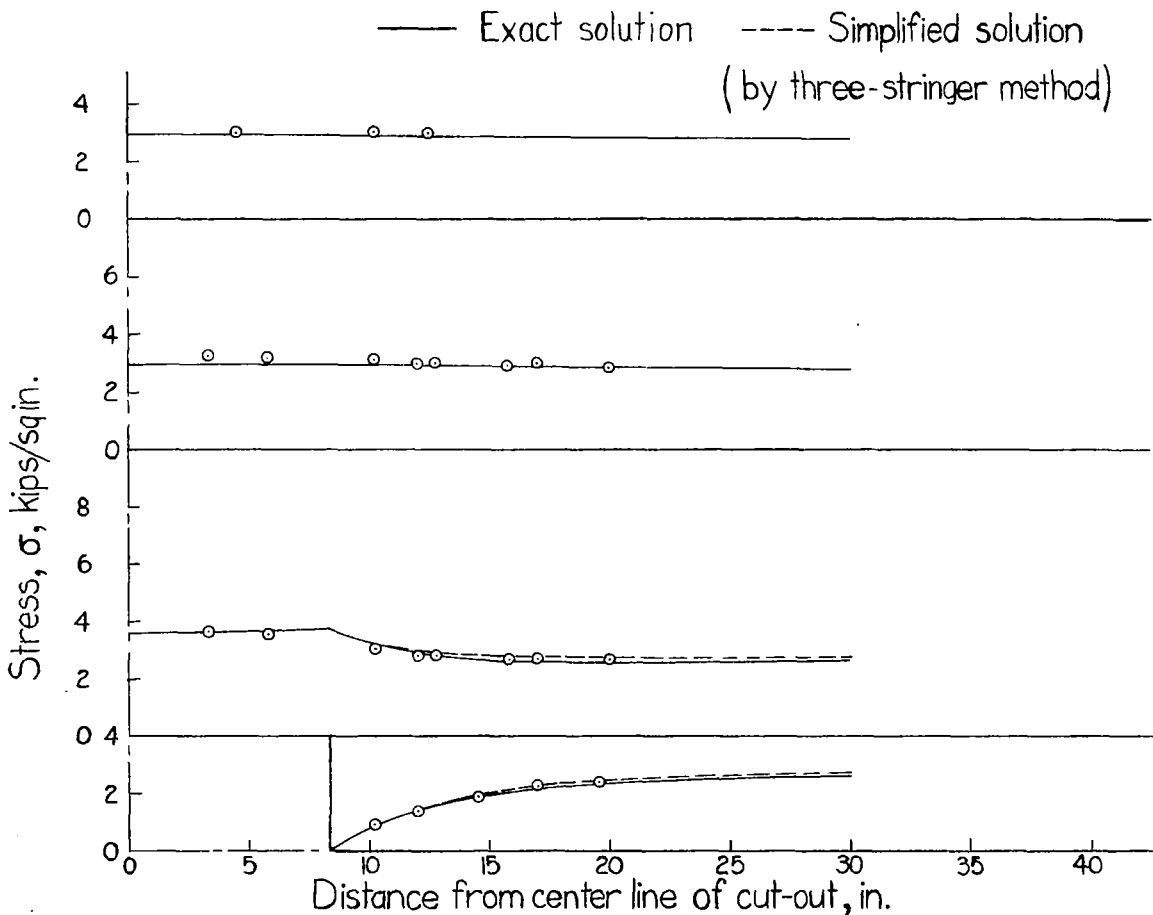


Figure 11.-Stringer stresses in 15-stringer panel with 1 stringer cut and  $L=8.3$  inches.

NACA

Fig. 12

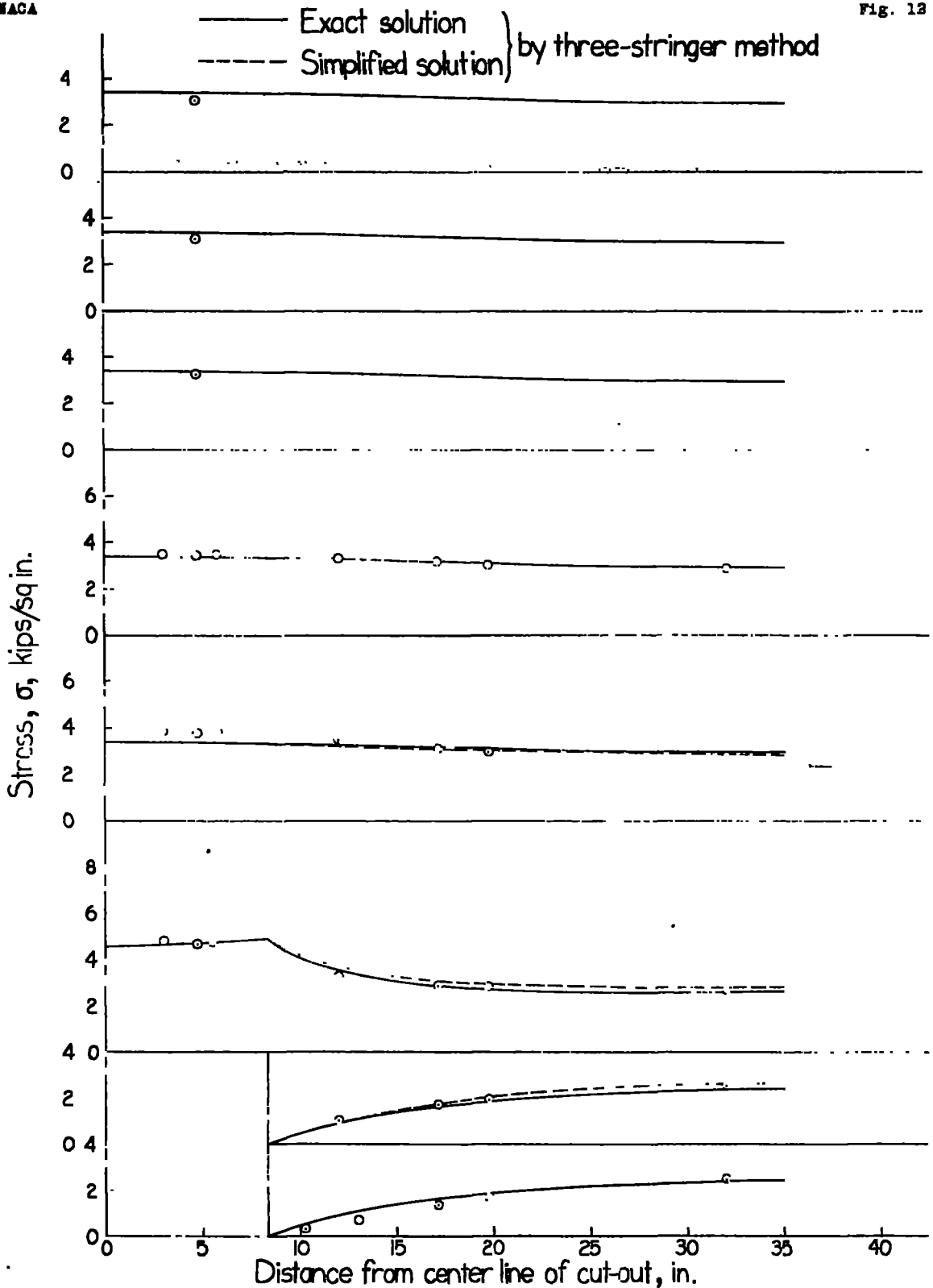


Figure 12.-Stringer stresses in 15-stringer panel with 3 stringers cut and  $L=8.3$  inches.

NACA

Fig. 13

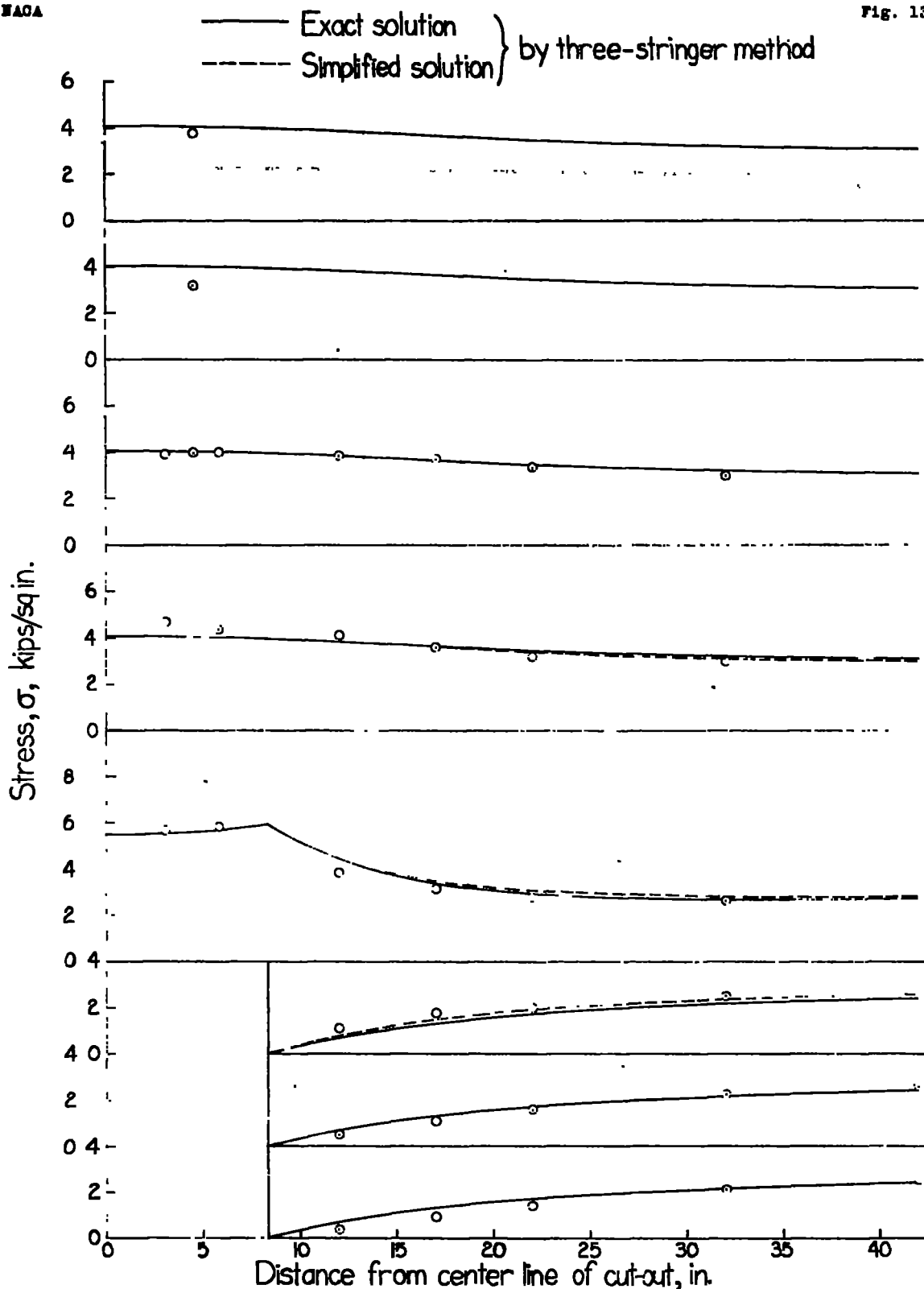


Figure 13.-Stringer stresses in 15-stringer panel with 5 stringers cut and  $L=8.3$  inches.

NACA

Fig. 14

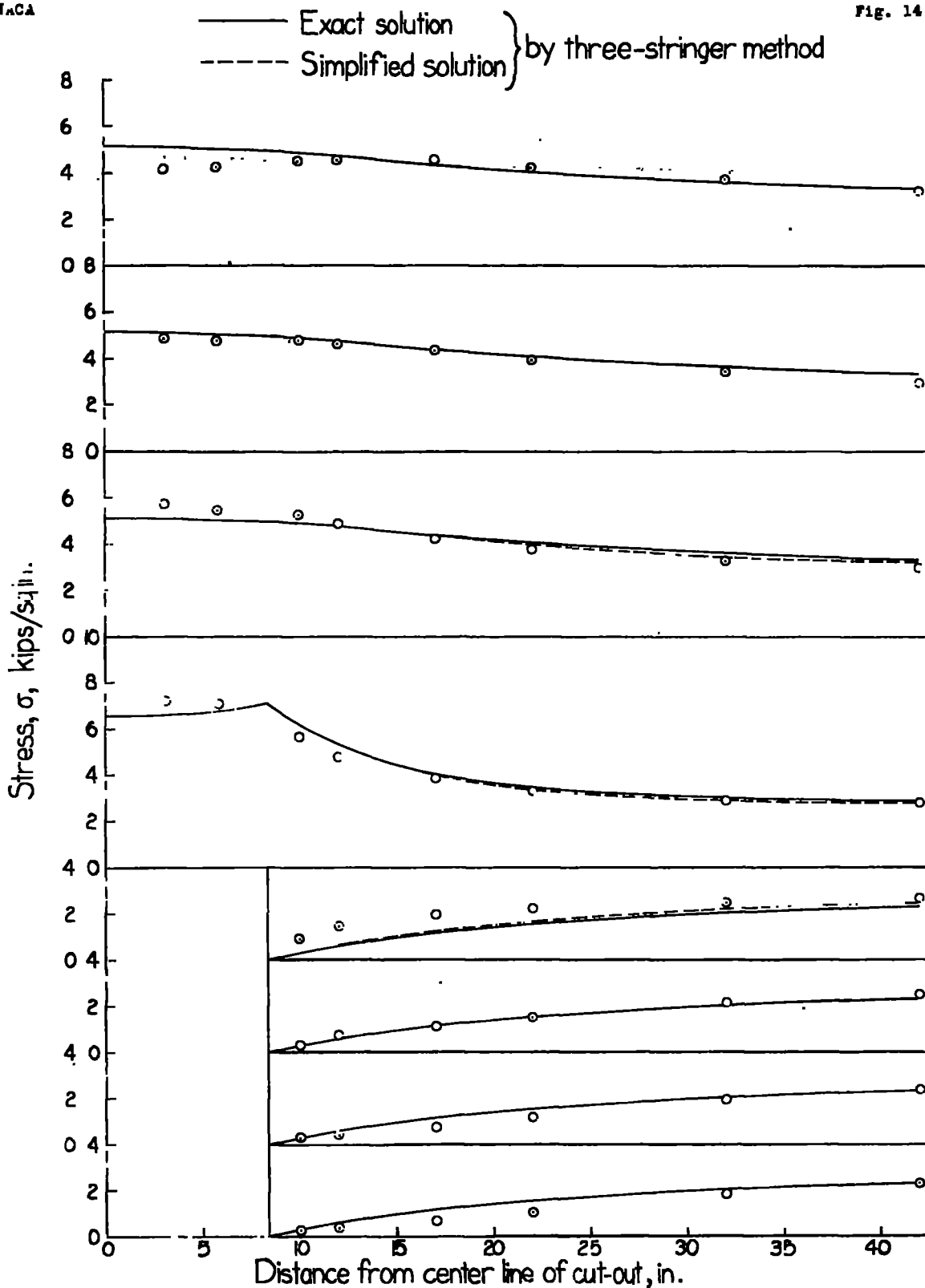


Figure 14.—Stringer stresses in 15-stringer panel with 7 stringers cut and  $L=8.3$  inches.

NACA

Fig. 15

— Exact solution } by three-stringer method  
 - - - Simplified solution

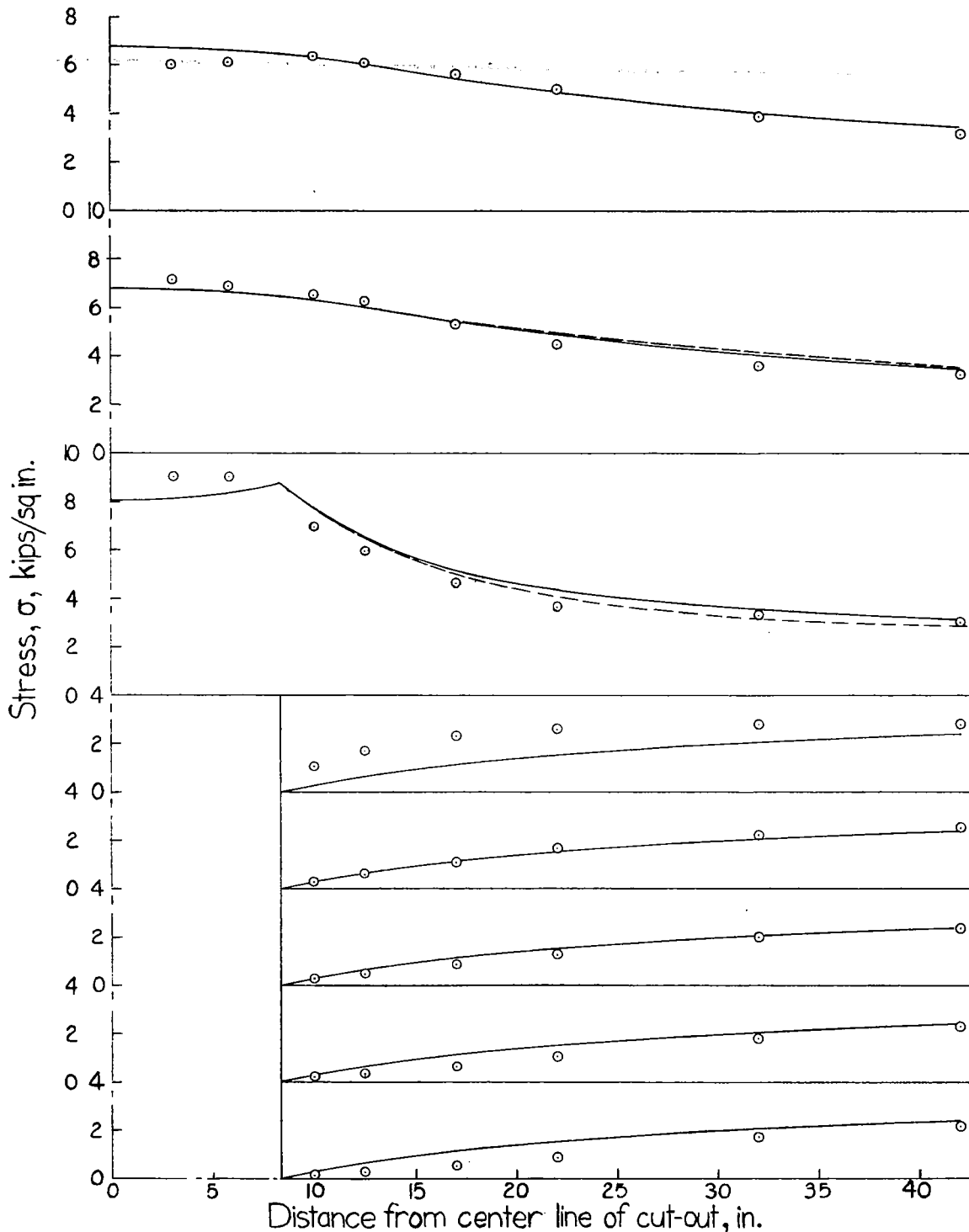


Figure 15.-Stringer stresses in 15-stringer panel with 9 stringers cut and  $L=8.3$  inches.

NACA

Fig. 16

— Exact solution  
 - - - Simplified solution } by three-stringer method

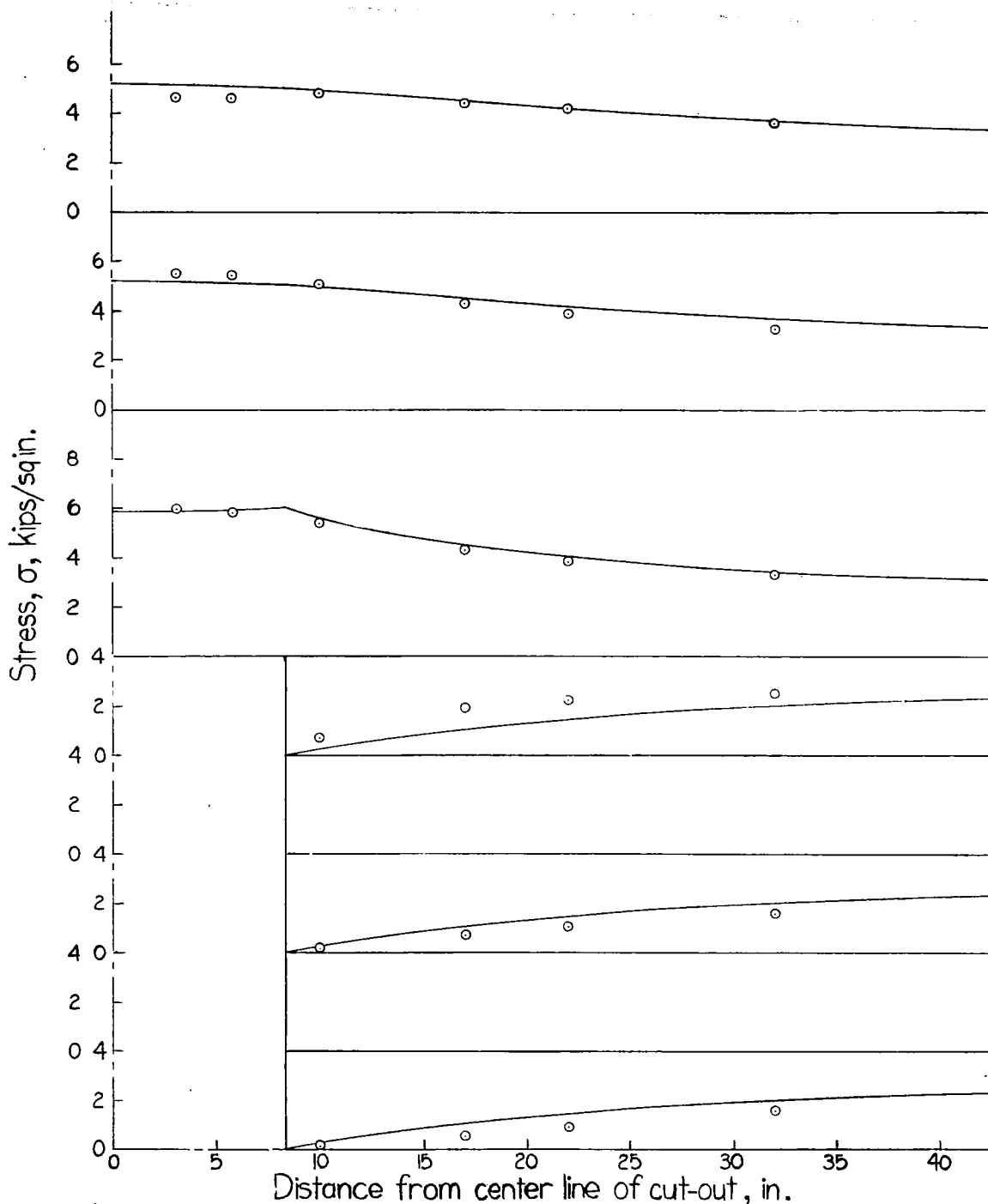


Figure 16.-Stringer stresses in 15-stringer panel with 9 stringers cut and  $L=8.3$  inches. Heavy main stringers.

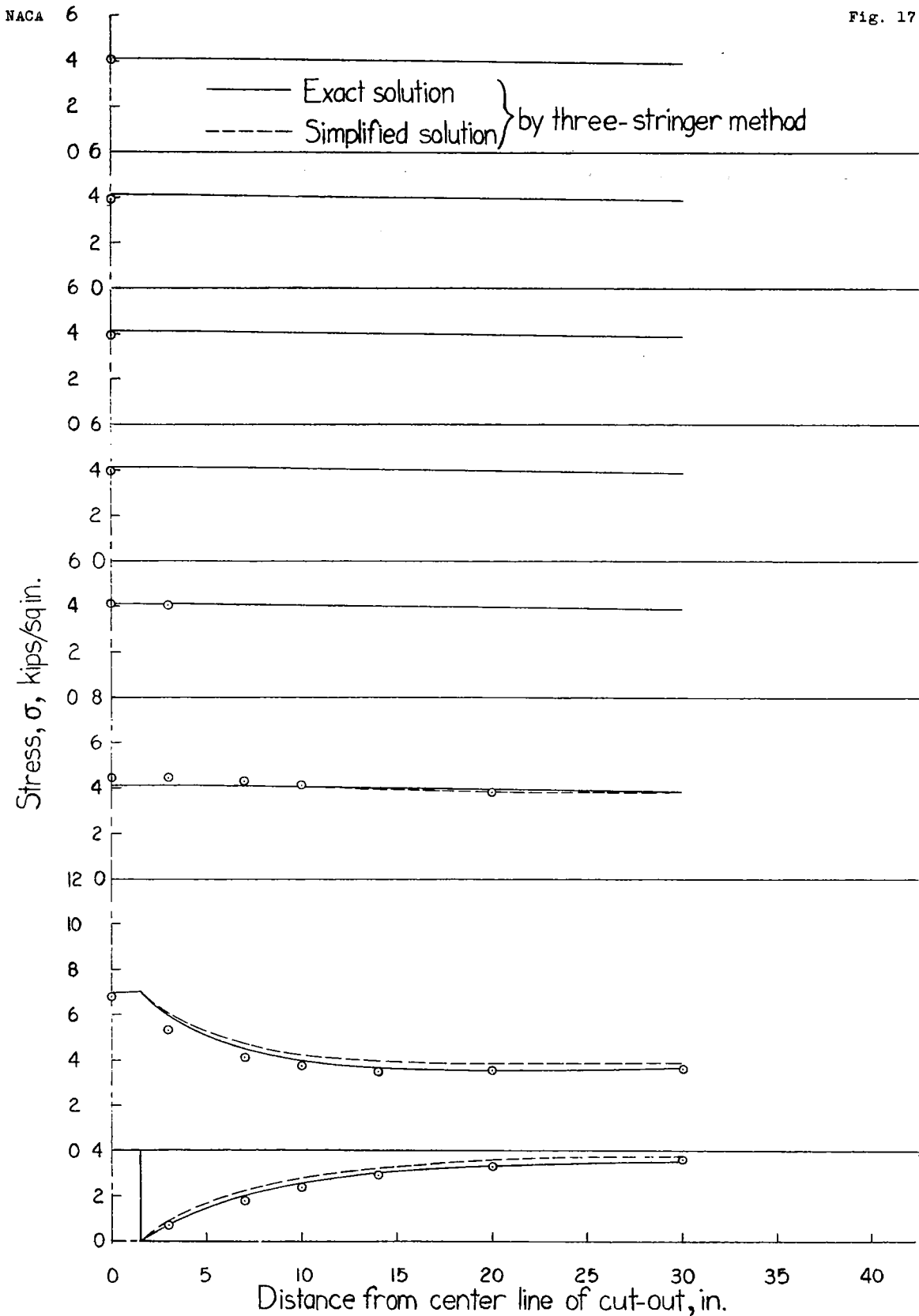


Fig. 17

Figure 17.-Stringer stresses in 16-stringer panel with 2 stringers cut and L=1.5 inches.

NACA

Fig. 18

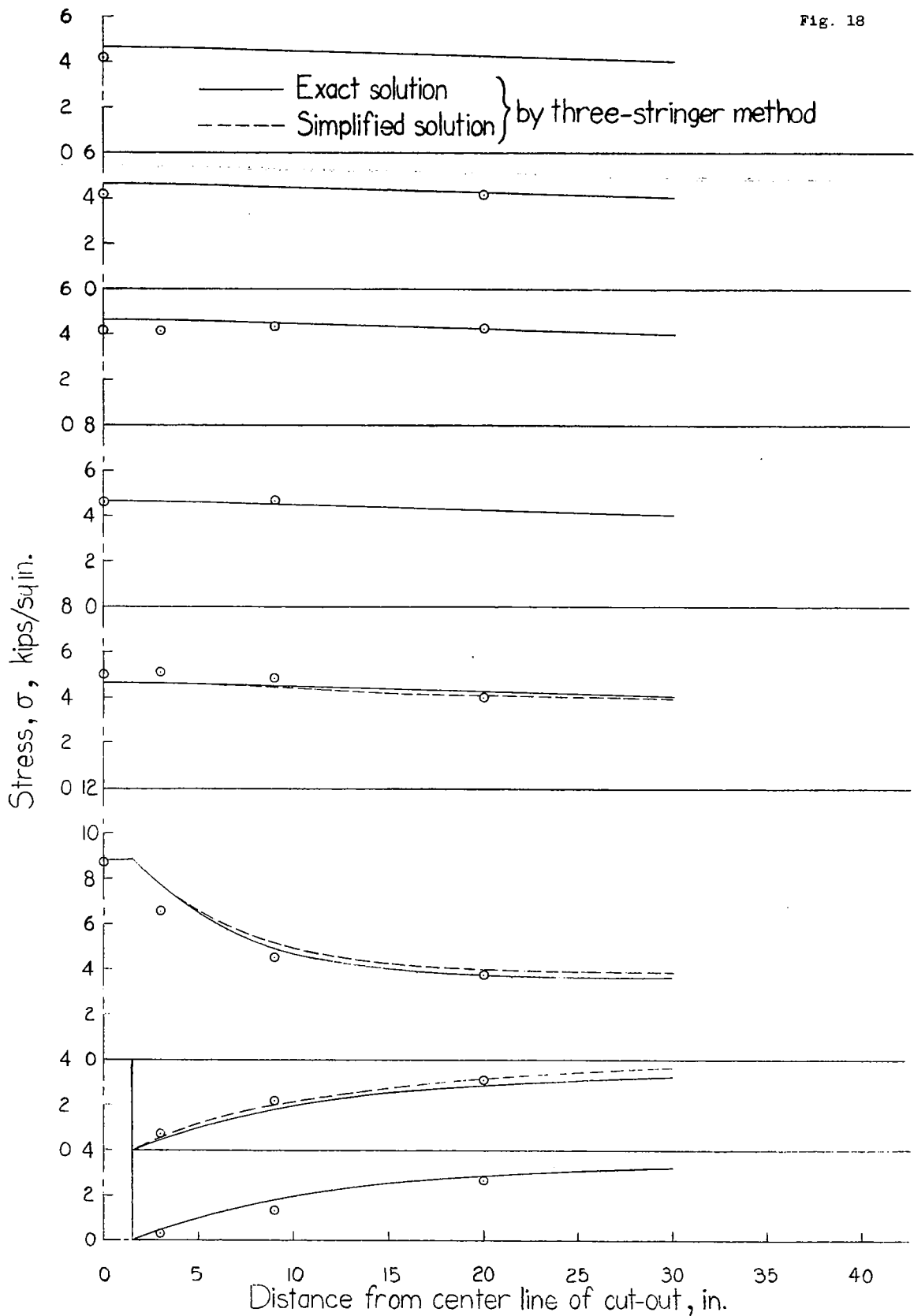


Figure 18.-Stringer stresses in 16-stringer panel with 4 stringers cut and  $L=1.5$  inches.

NACA

Fig. 19

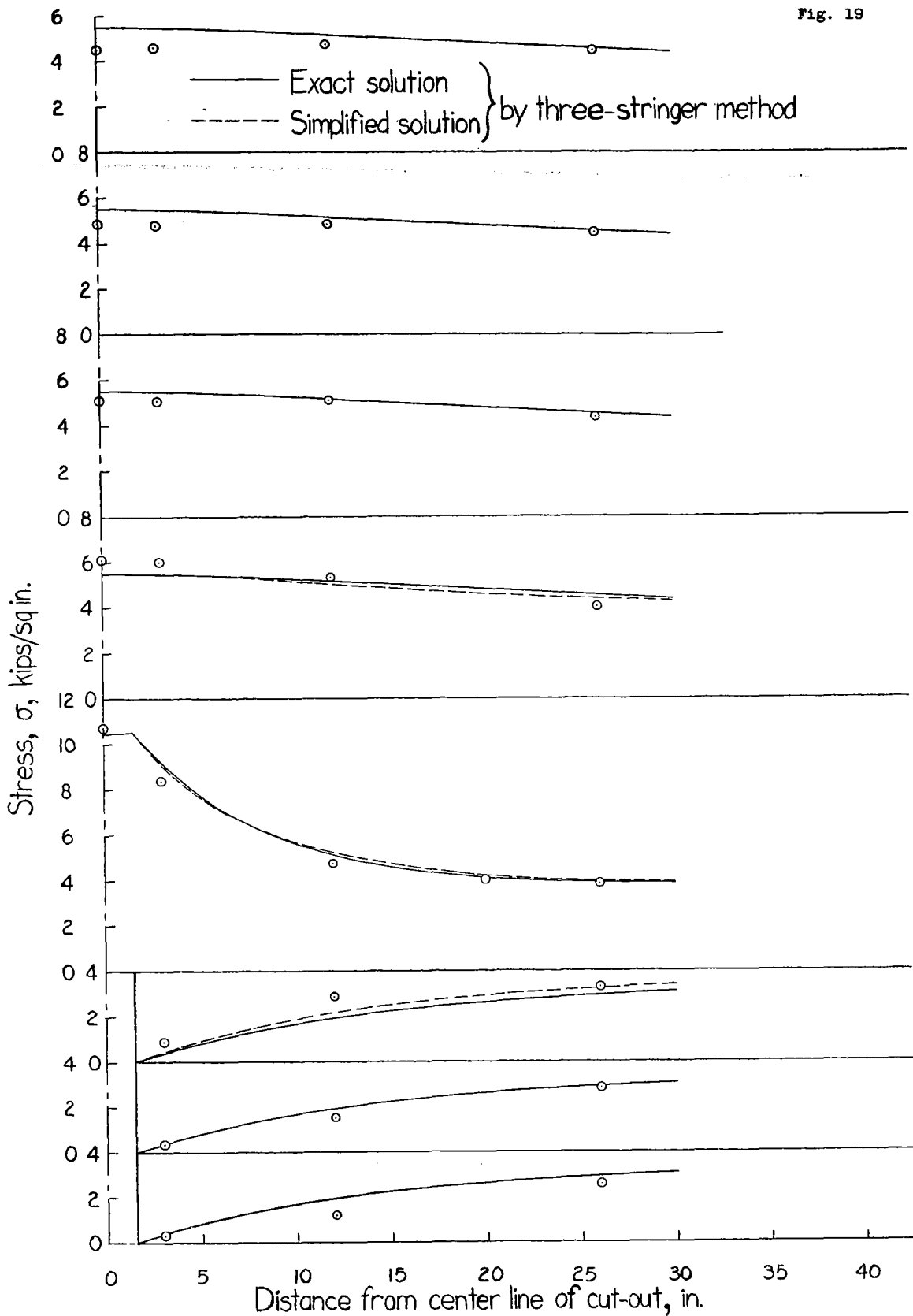


Figure 19.-Stringer stresses in 16-stringer panel with 6 stringers cut and  $L=1.5$  inches.

NACA

Fig. 20

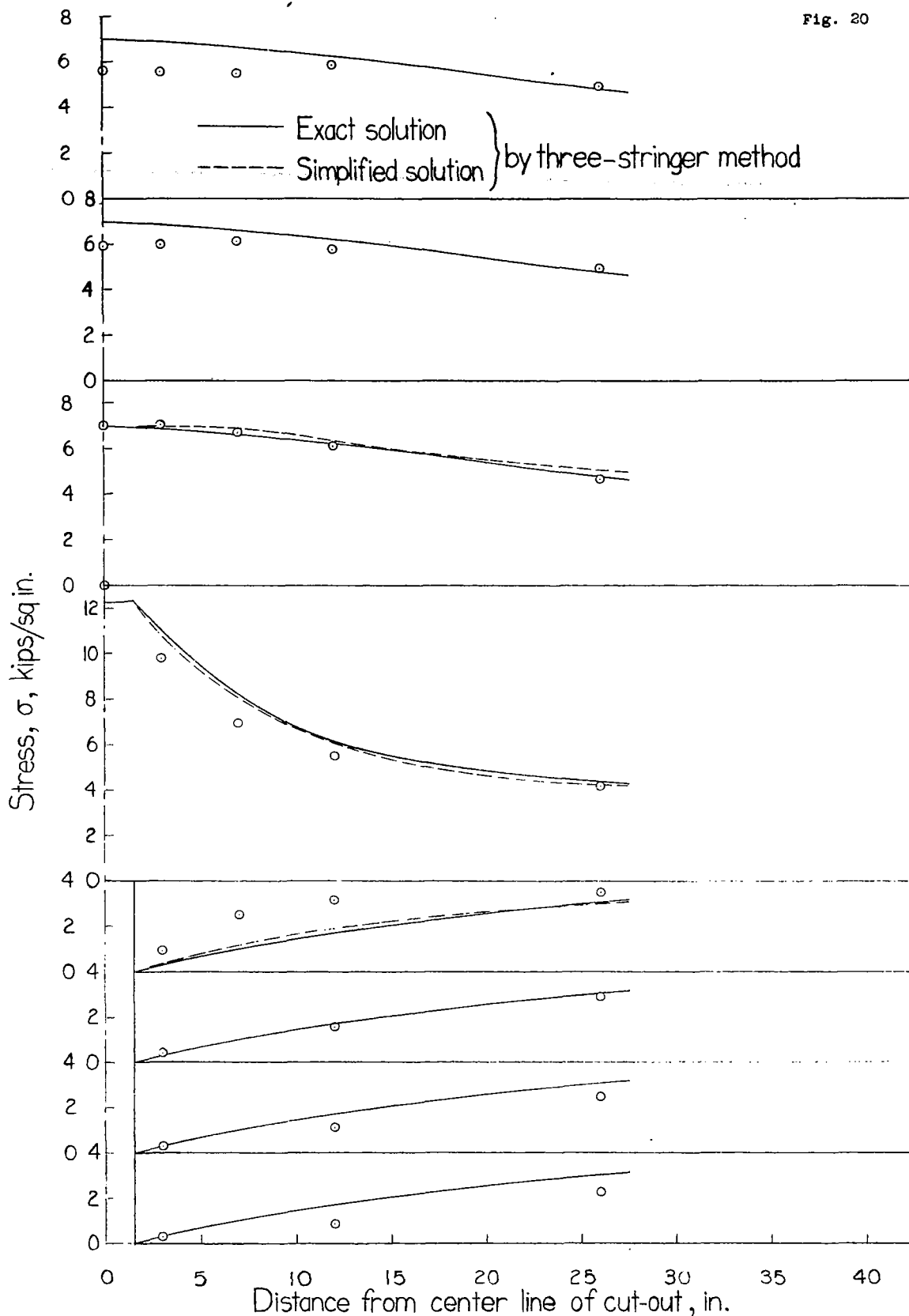


Figure 20.-Stringer stresses in 16-stringer panel with 8 stringers cut and L=15 inches.

NACA

Fig. 21

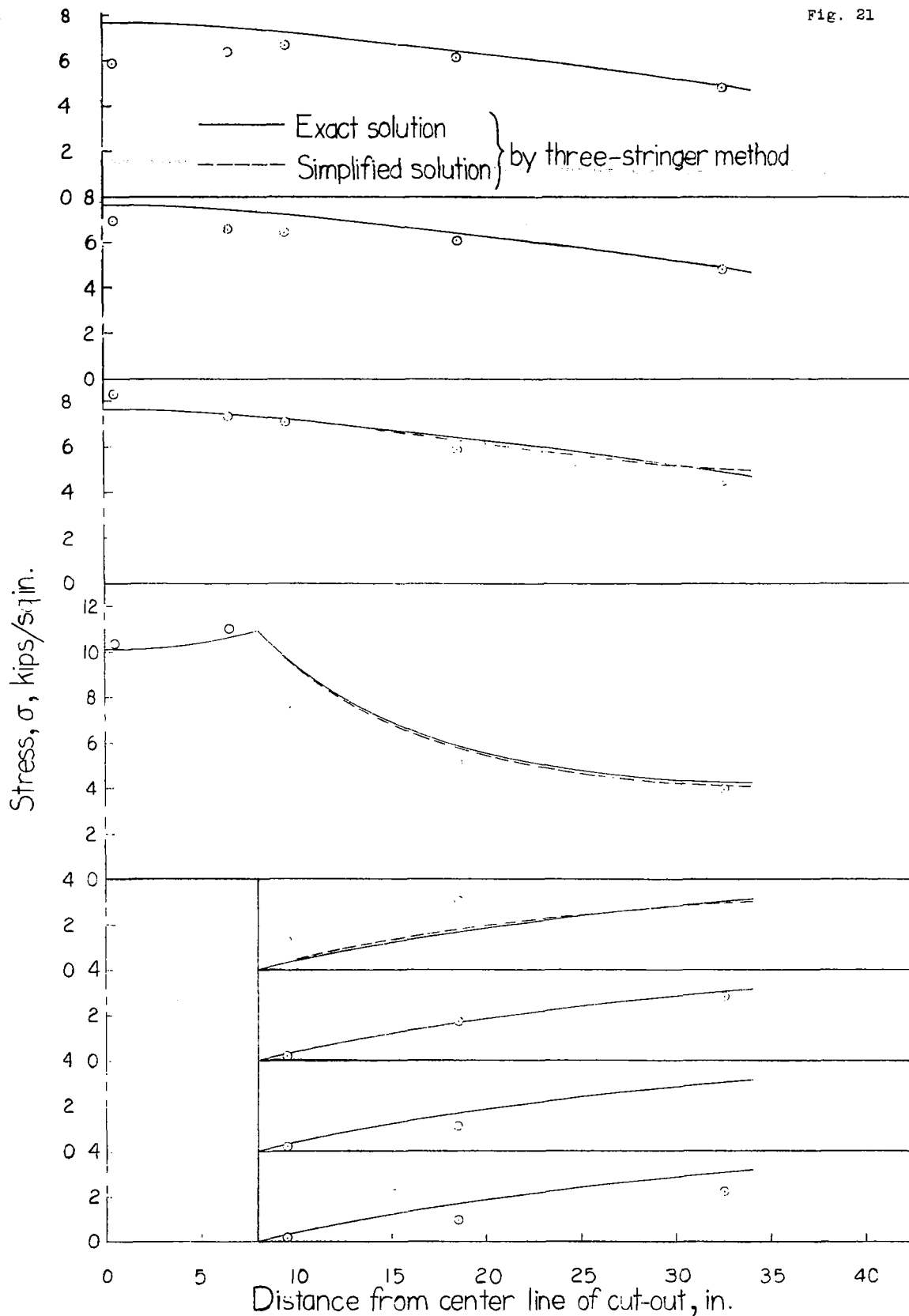


Figure 21.-Stringer stresses in 16-stringer panel with 8 stringers cut and  $L=8.0$  inches.

NACA

Fig. 22

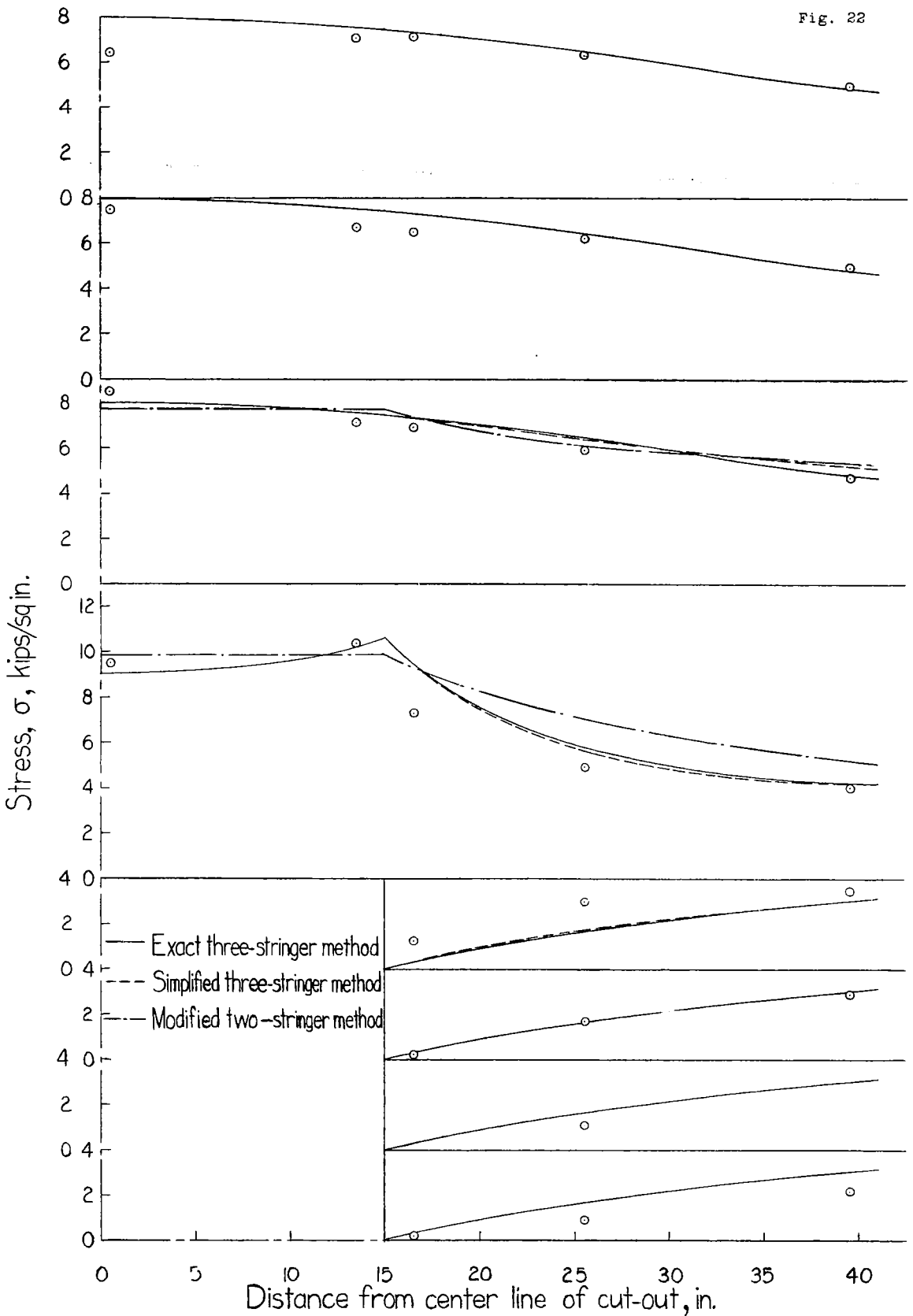


Figure 22.-Stringer stresses in 16-stringer panel with 8 stringers cut and  $L=15.0$  inches.

NACA

Fig. 23

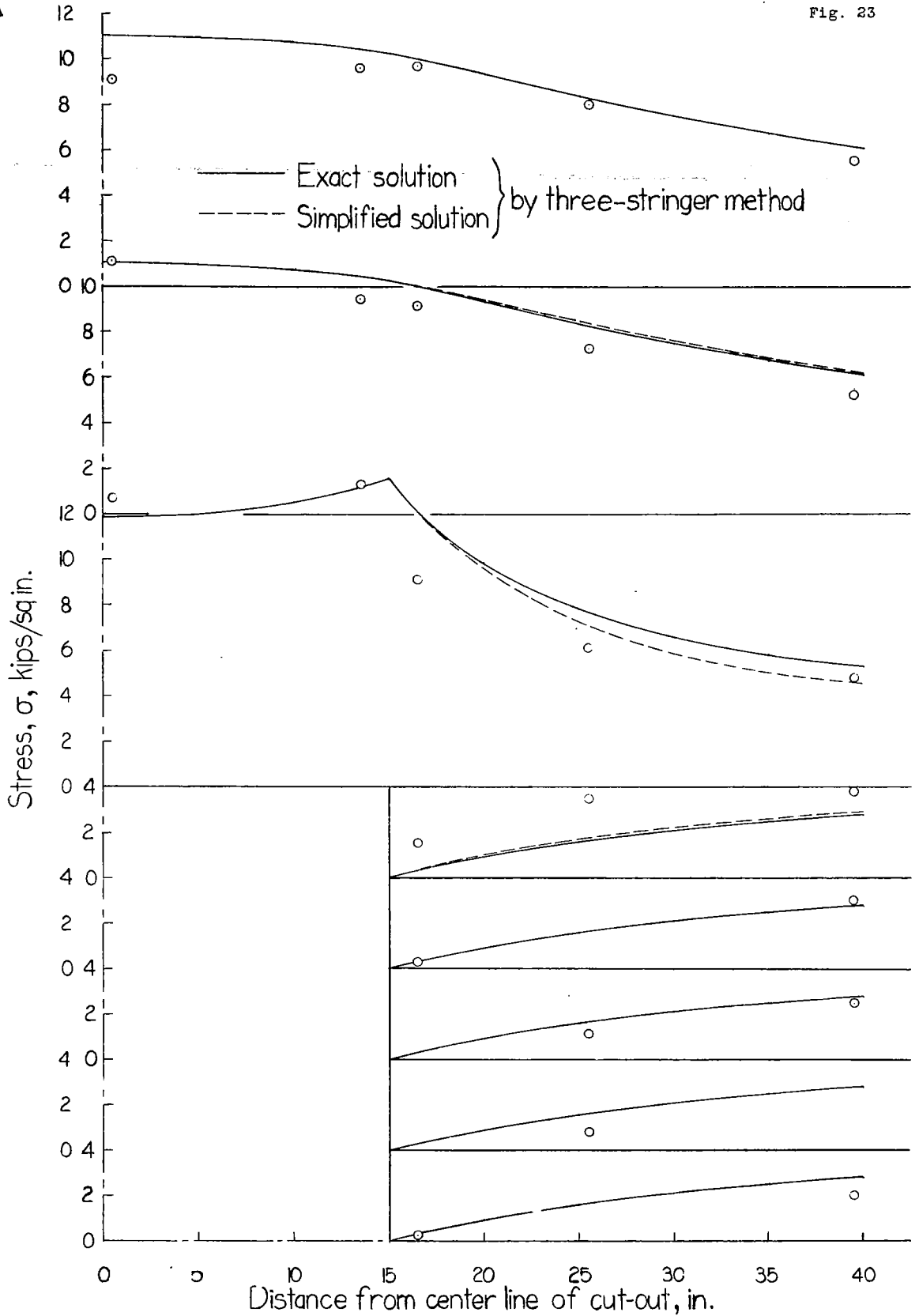


Figure 23: Stringer stresses in 16-stringer panel with 10 stringers cut and  $L=15.0$  inches.

NACA

Fig. 24

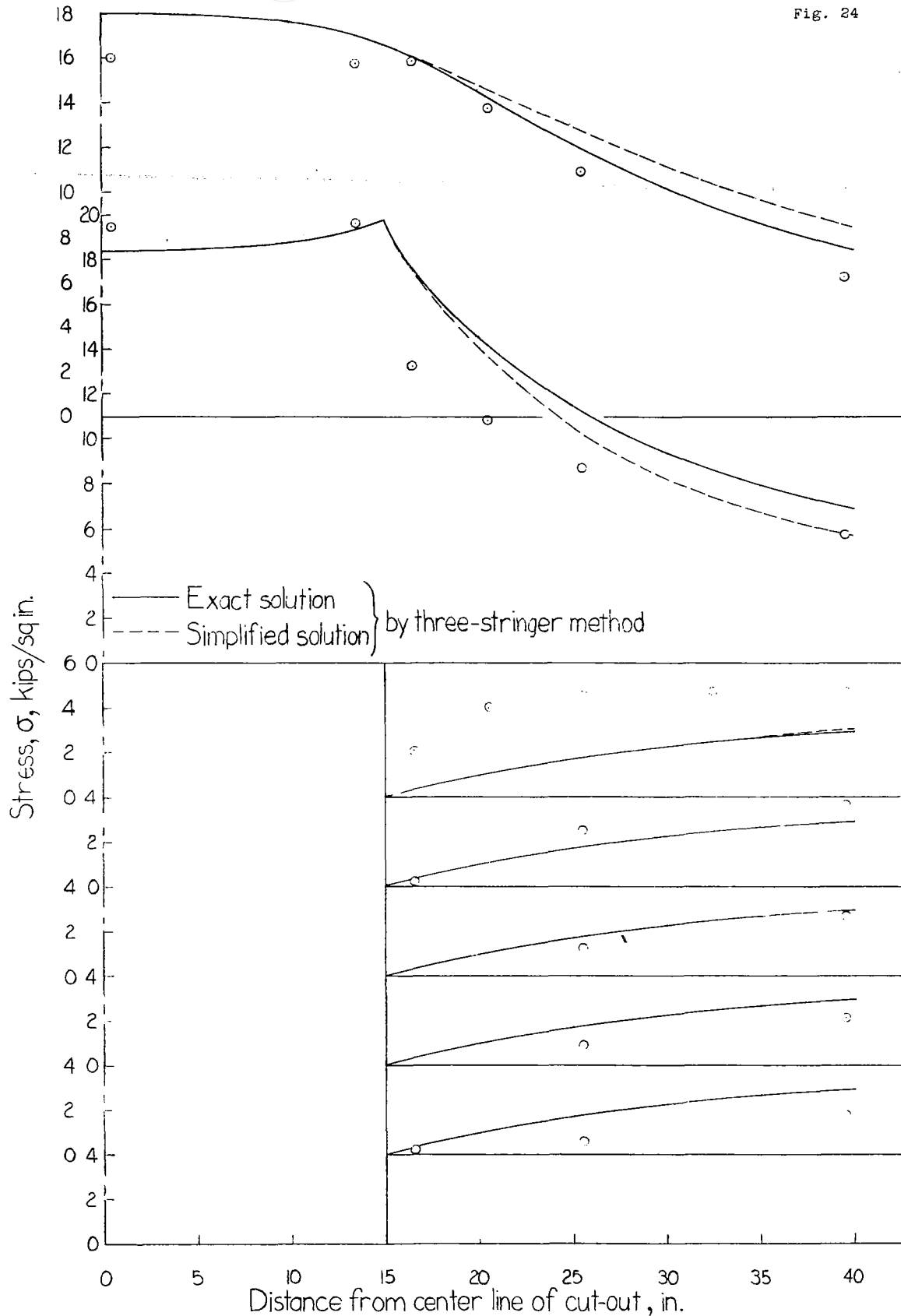


Figure 24.-Stringer stresses in 16 stringer panel with 12 stringers cut and  $L=15.0$  inches.

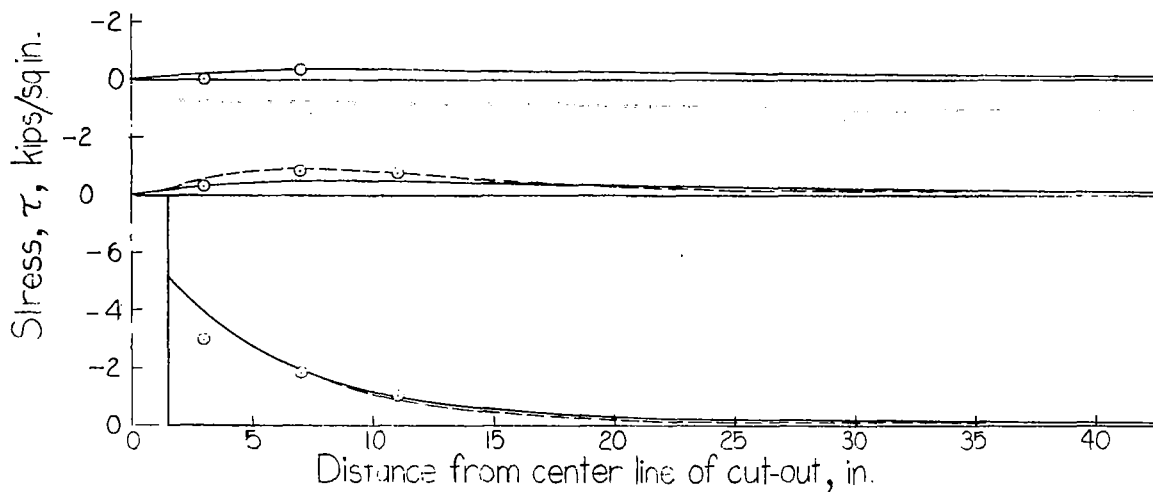


Figure 25.-Shear stresses in 16-stringer panel with 2 stringers cut and  $L=1.5$  inches.

— Exact solution  
 ---- Simplified solution  
 (by three-stringer method)

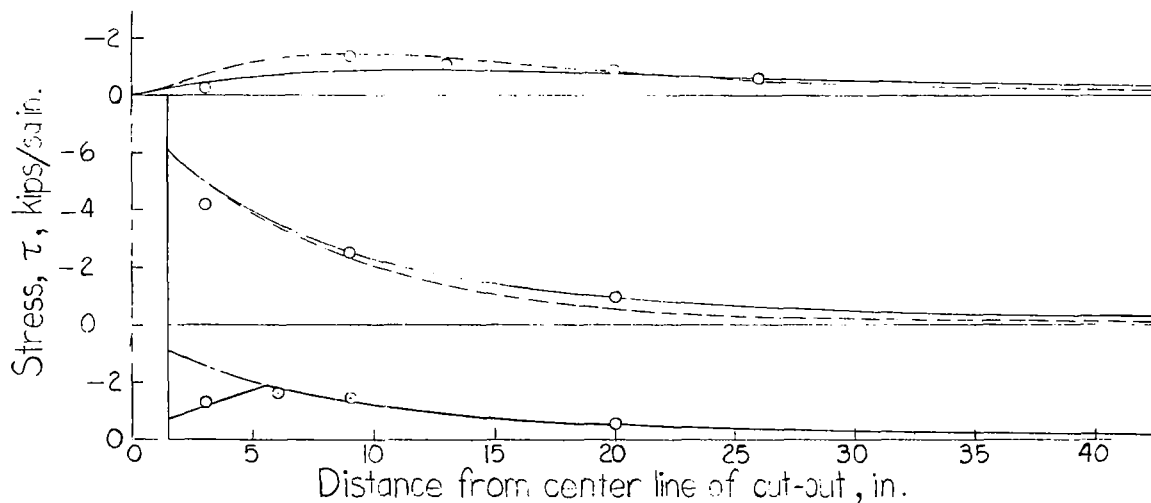


Figure 26.-Shear stresses in 16-stringer panel with 4 stringers cut and  $L=1.5$  inches.

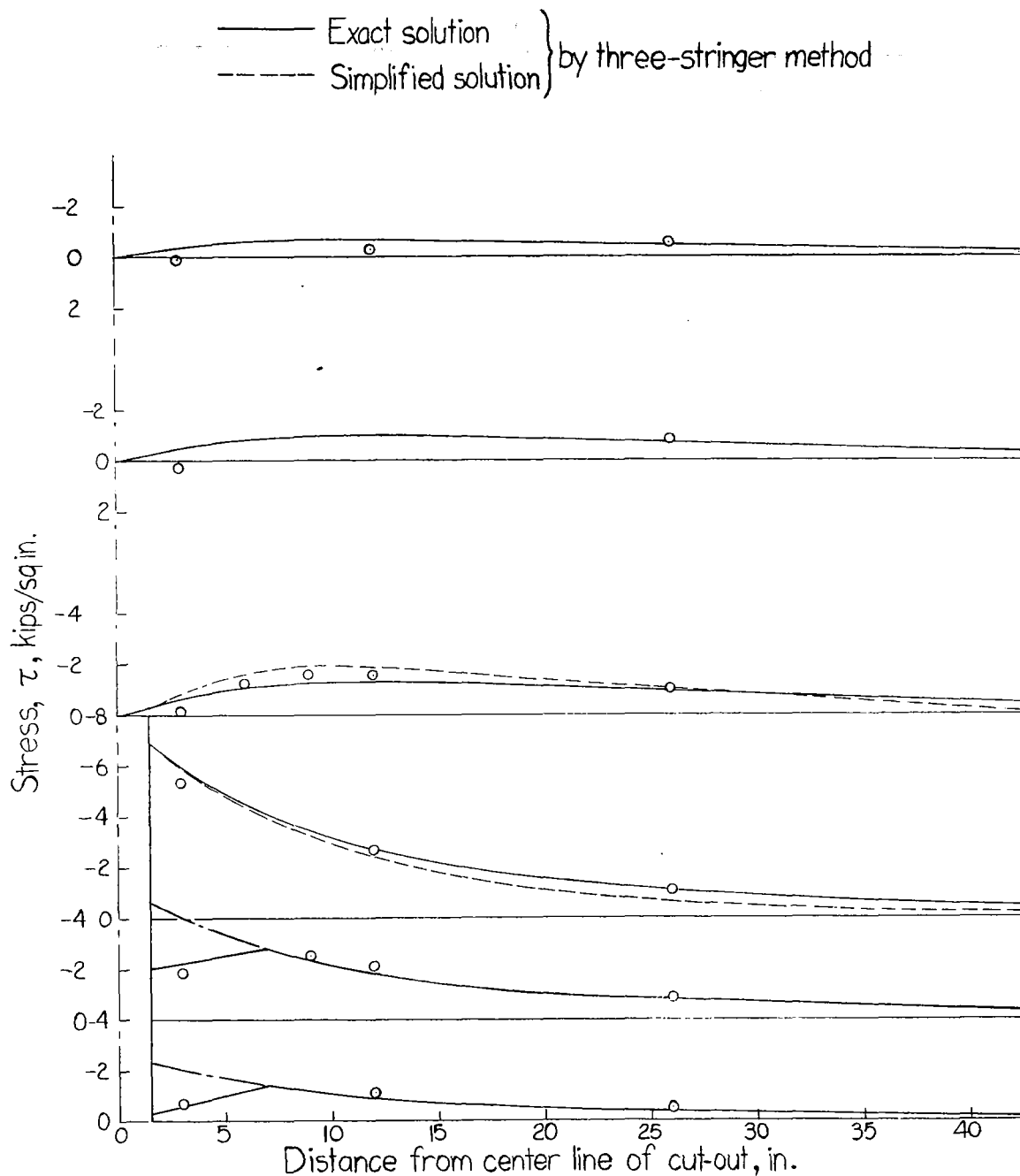


Figure 27.-Shear stresses in 16-stringer panel with 6 stringers cut and  $L=1.5$  inches.

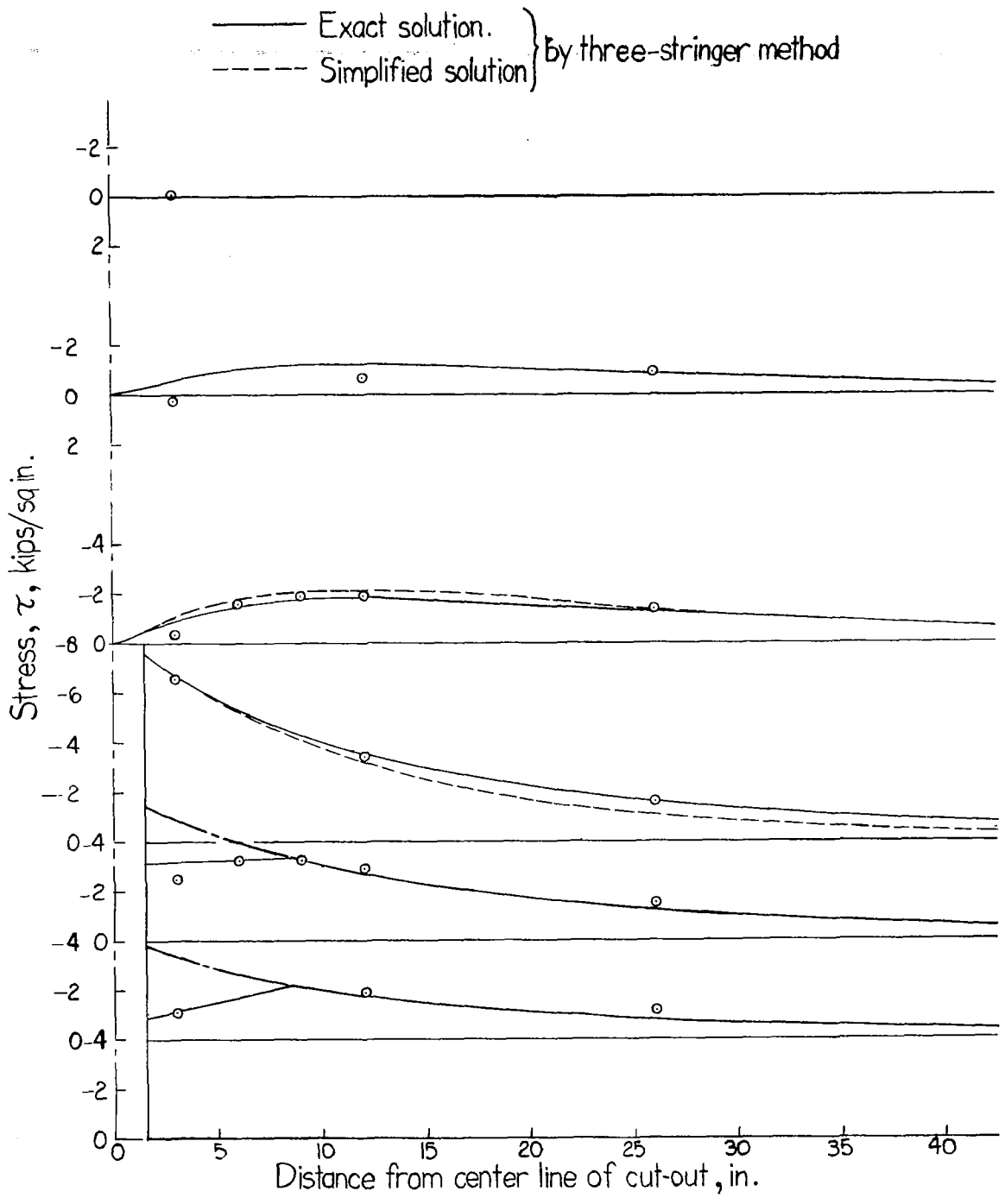


Figure 28.—Shear stresses in 16-stringer panel with 8 stringers cut and  $L=1.5$  inches.

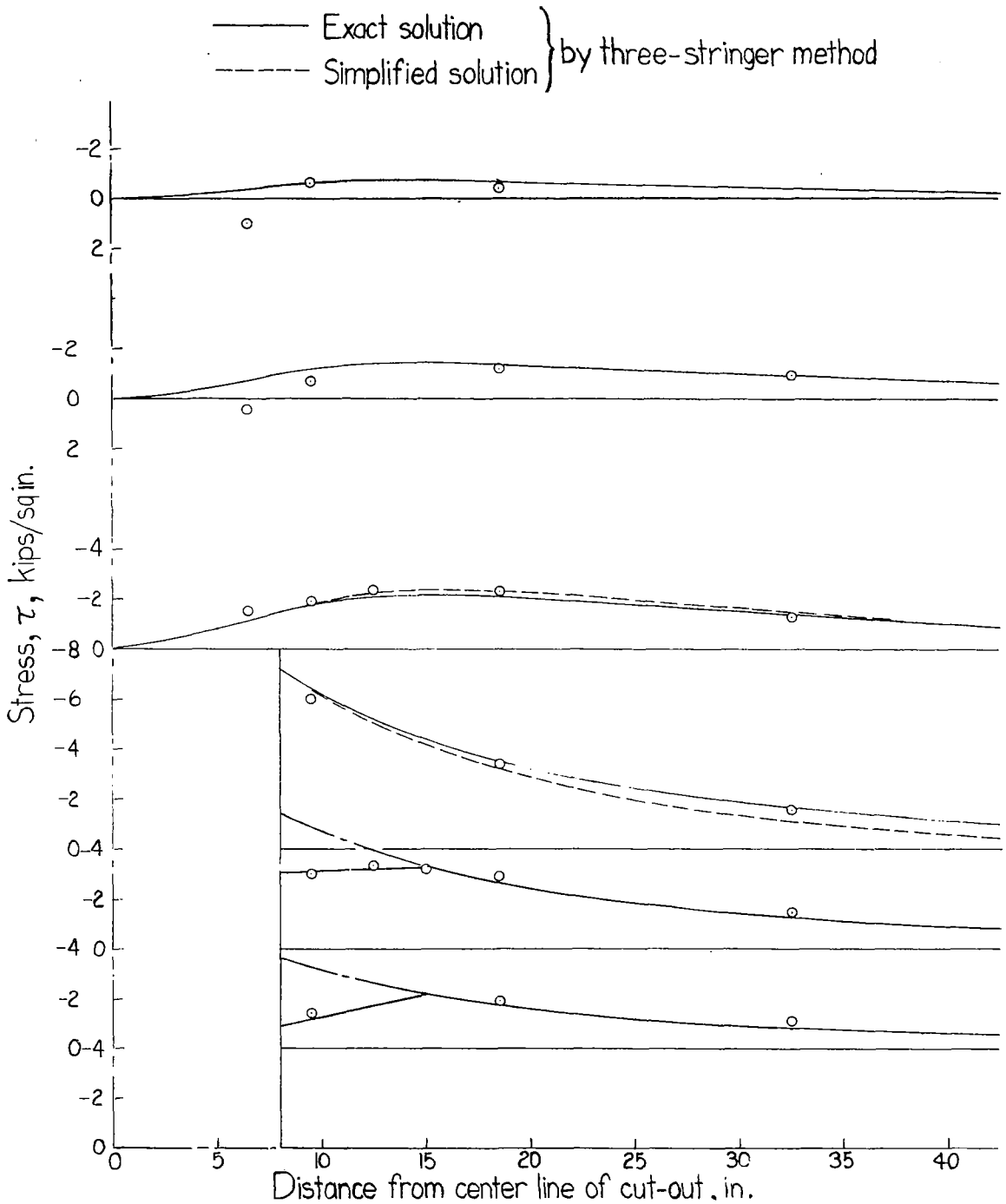


Figure 29.- Shear stresses in 16-stringer panel with 8 stringers cut and  $L = 8.0$  inches.

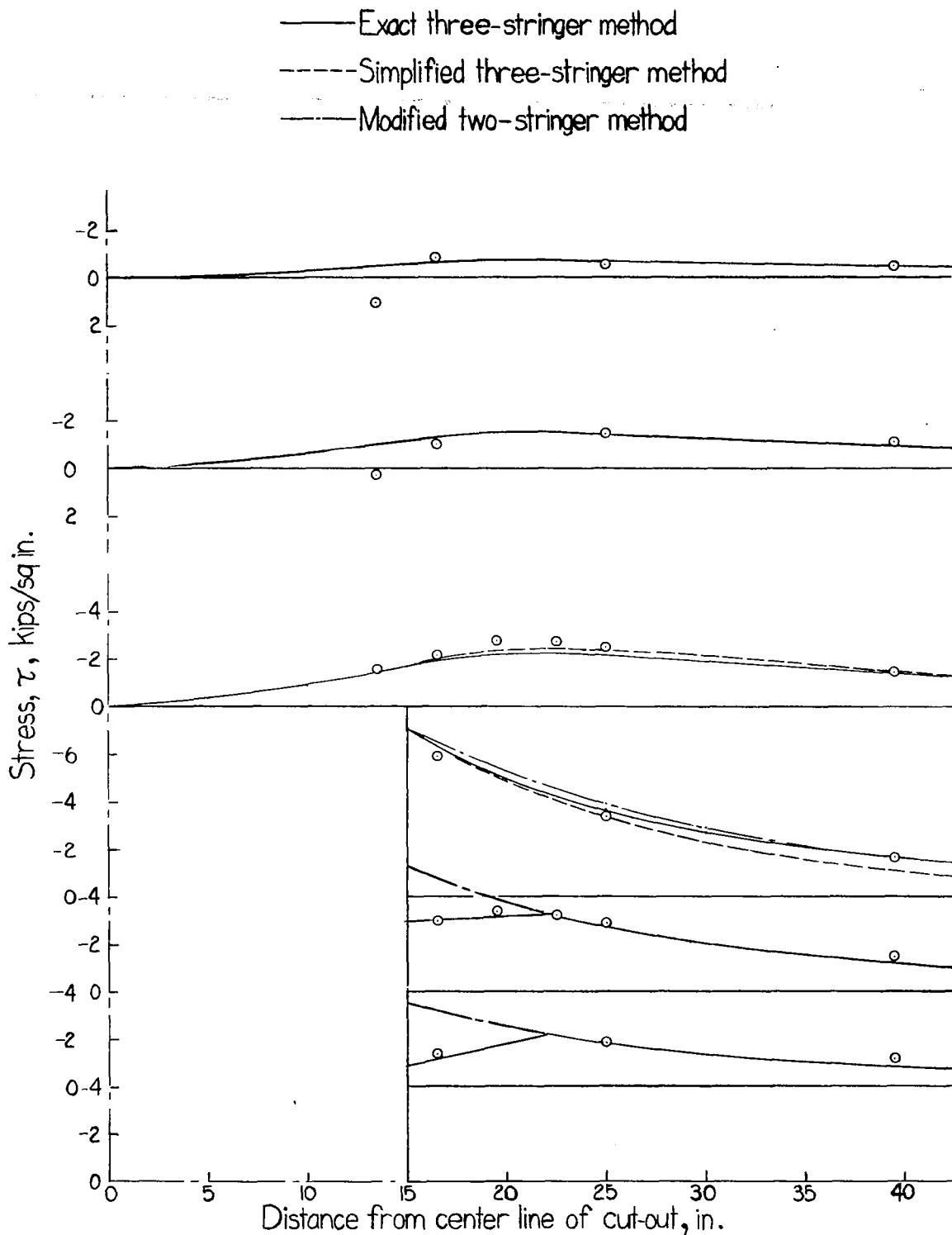


Figure 30. Shear stresses in 16-stringer panel with 8 stringers cut and  $L=15.0$  inches.

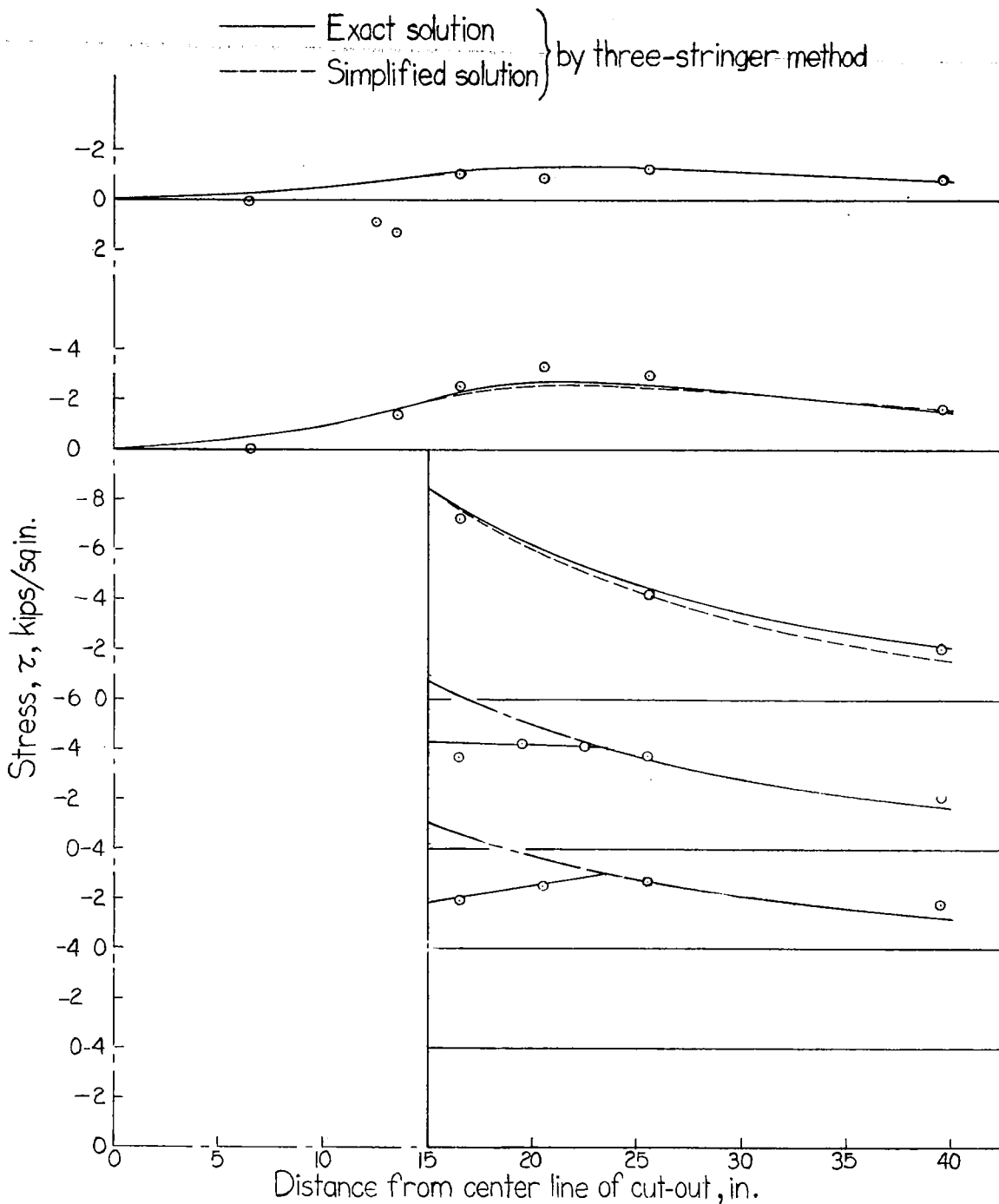


Figure 31.-Shear stresses in 16-stringer panel with 10 stringers cut and  $L=15.0$  inches.

NACA

Fig. 32

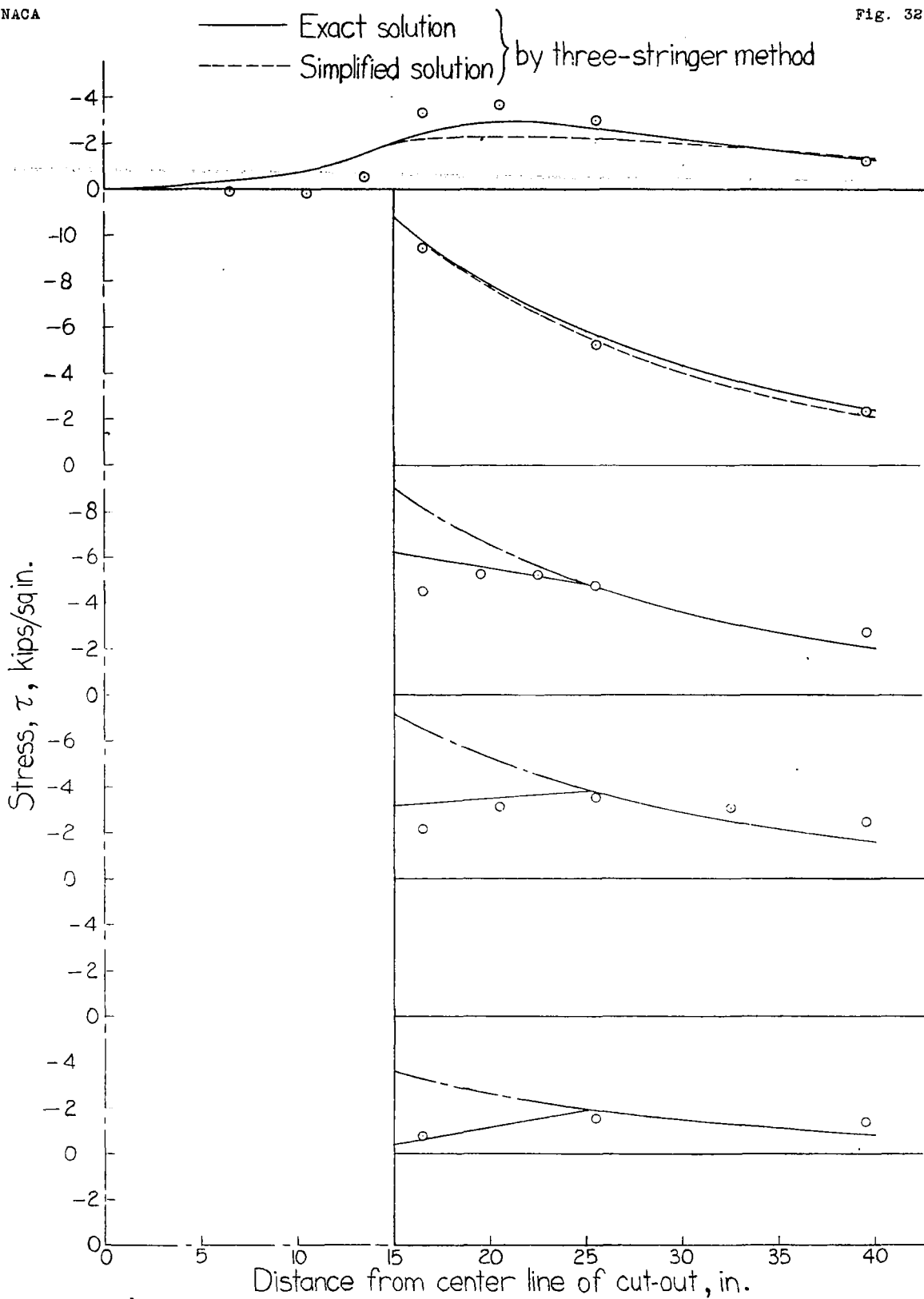
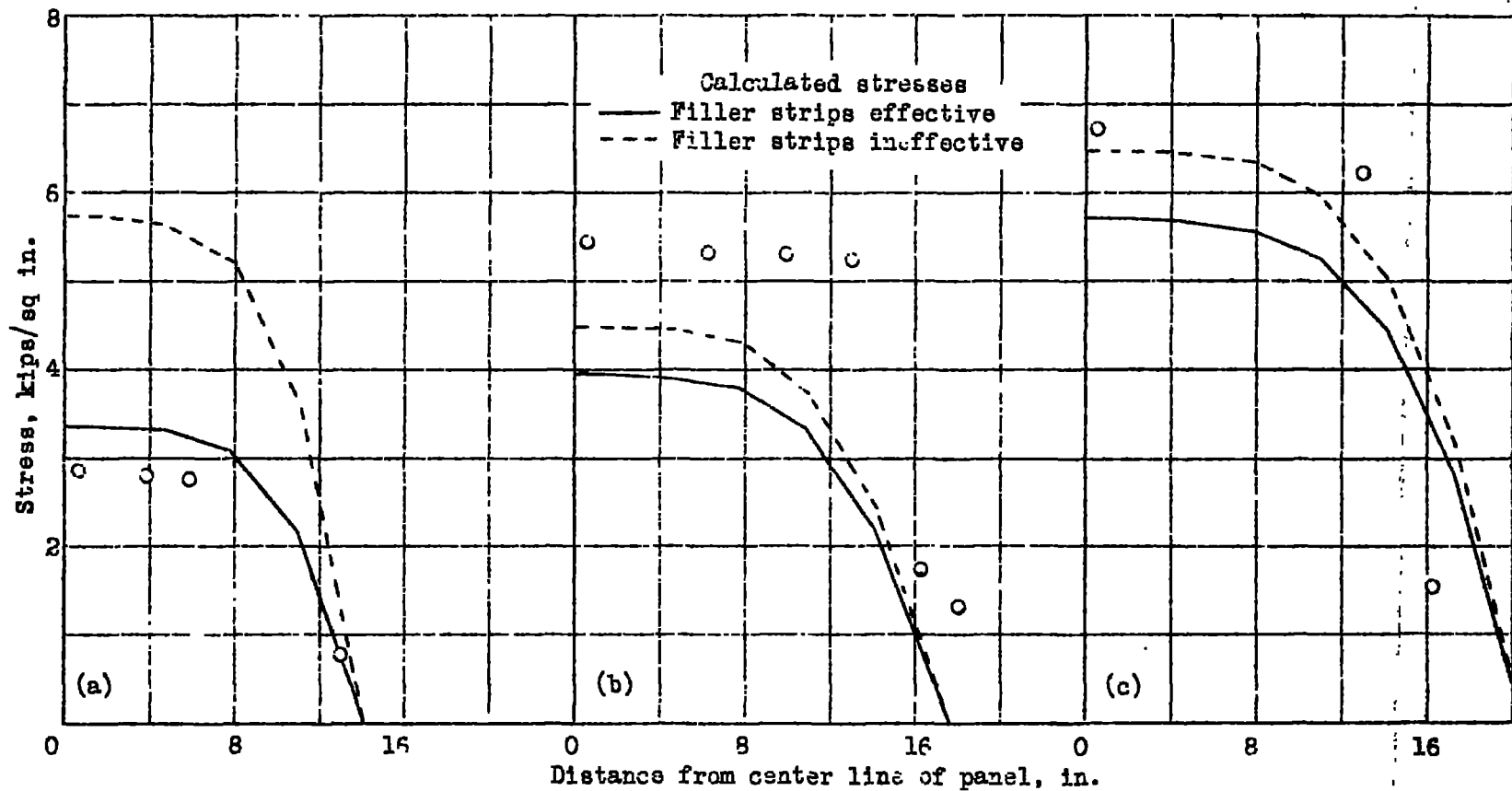


Figure 32.-Shear stresses in 16-stringer panel with 12 stringers cut and  $L=15.0$  inches.



- (a) 16-stringer panel; 8 stringers cut;  $L = 1.5$  inches.
- (b) 16-stringer panel; 10 stringers cut;  $L = 15.0$  inches.
- (c) 16-stringer panel; 12 stringers cut;  $L = 15.0$  inches.

Figure 33.- Experimental and calculated rib stresses. Panel load = 15 kips.

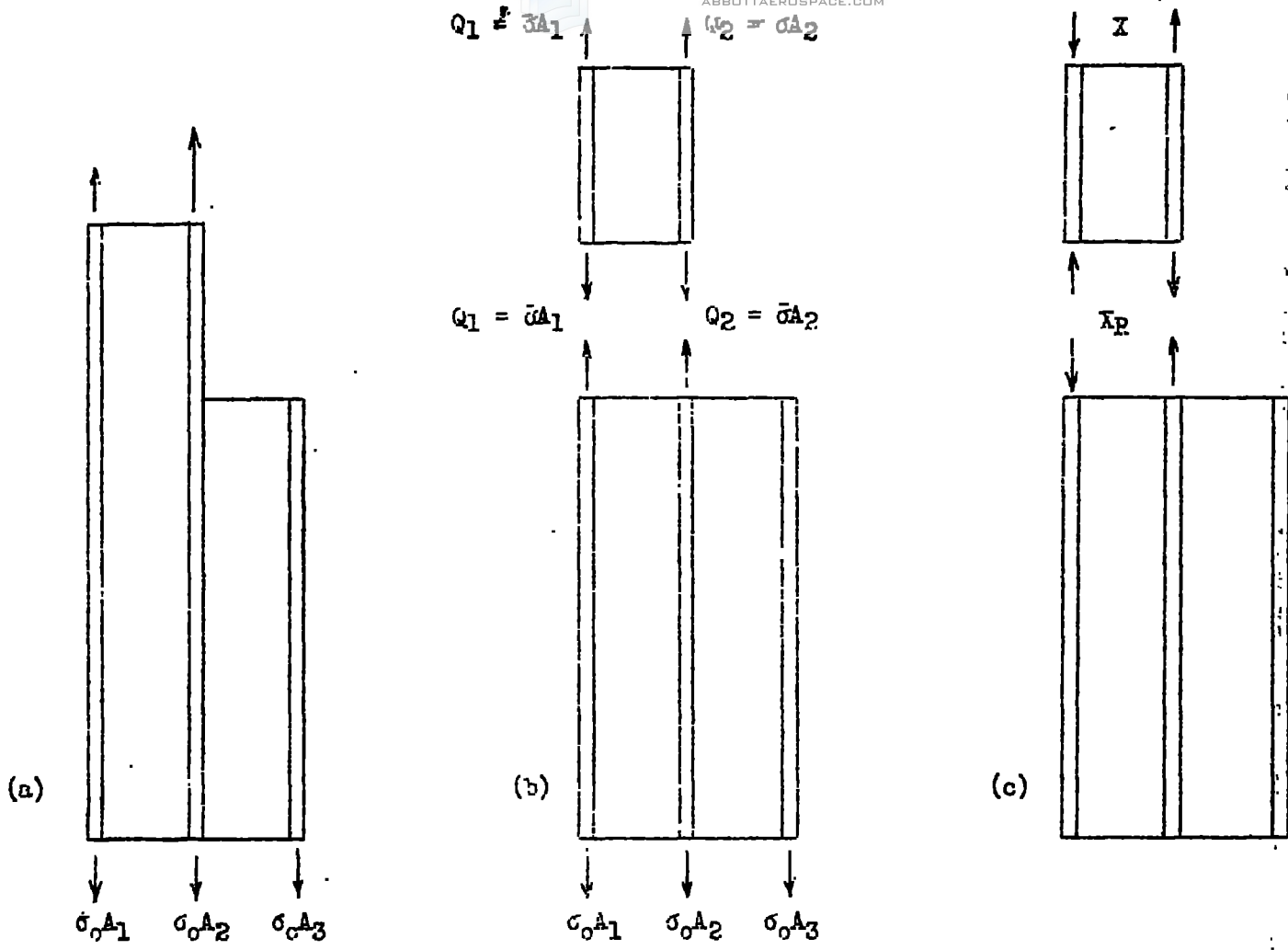


Figure 34.- Resolution of loads on three-stringer structure.